FAKULTA MATEMATIKY, FYZIKY A INFORMATIKY

UNIVERZITY KOMENSKÉHO

V BRATISLAVE

KATEDRA BIOFYZIKY A CHEMICKEJ FYZIKY

D I P L O M O V Á P R Á C A

2003 Kristína Šušmáková

FAKULTA MATEMATIKY, FYZIKY A INFORMATIKY

UNIVERZITY KOMENSKÉHO

V BRATISLAVE

KATEDRA BIOFYZIKY A CHEMICKEJ FYZIKY

NELINEÁRNA ŠTATISTICKÁ ANALÝZA DYNAMIKY ĽUDSKEJ CHÔDZE

Diplomová práca

Vedúci dipl. práce : Doc. RNDr Peter Babinec, CSc.

Kristína Šušmáková

2003

Prehlasujem, že som túto prácu vypracovala samostatne, za odbornej pomoci svojho diplomového vedúceho a s použitím literatúry uvedenej v zozname.

Bratislava, 2003

Ďakujem môjmu diplomovému vedúcemu Doc. RNDr. Petrovi Babincovi za pomoc pri tvorbe tejto práce, za odborné rady a povzbudenie.

FACULTY OF MATHEMATICS, PHYSICS AND INFORMATICS

COMENIUS UNIVERSITY

BRATISLAVA

DEPARTMENT OF BIOPHYSICS AND CHEMICAL PHYSICS

NONLINEAR STATISTICAL ANALYSIS OF HUMAN GAIT DYNAMICS

MSc thesis

Supervisor: Doc. RNDr. P. Babinec, CSc. **Kristína Šušmáková**

2003

CONTENTS

Introduction

The popularity of chaos theory, judged by the number of scientific publications and by the attention of media, has a dangerous drawback in that it could be seen as the answer to everything, something that is obviously not. An example of this oversimplification is to be found in the phenomenon of turbulence in fluid flows. Over the past decade the words chaos and turbulence have become almost synonymous in many popular accounts and yet the connection between the two is far from obvious even today. Common opinion is that the ideas of chaos have thus far added very little to the understanding of the phenomenon of turbulence. However, chaos seems to have survived the fashionable phase and perhaps one reason is that the natural world is inherently non-linear. Therefor, one should expect to find chaos rather than order and perhaps we now have some tools for furthering our understanding of what was previously thought of as random noise. There are many deep mathematical ideas behind the dynamical systems approach to the study of nonlinear phenomena which are aimed at describing and understanding the origins and structures of complicated behavior.

Naturally, there has been tendency to extend some of these ideas into fields where is no rigorous justification for doing so. There are often resolute efforts to tackle very difficult problems with new scientific ideas. The very last that one can say is that non-linearity should play a key role in natural phenomena and therefore some of these modern concepts may well give a new insight into some unresolved problems. On the other hand it is also worth noting that an irregular time series formed from ice core samples or the monitoring of bodily function for example need not necessarily be describable in terms of low-dimensional chaos. Therefore one must remain cautious about such studies for it is quite easy to misrepresent the above ideas by an imprecise application of techniques which have thus far only been successfully tested in well-controlled laboratory situations. However, if new insights into difficult areas are obtained using this approach, which amount to more than putting common sense into fancy mathematical language, then a great deal has been achieved.

In the recent decades the chaos theory was applied into physiological systems. It was discovered that randomness and unpredictability are characteristic features for healthy and young organisms, while ill people exhibit some regular structures. Our aim in this thesis is to apply various nonlinear techniques developed recently to the study of human locomotion. The locomotion is driven by nervous system in complex manners.

Information flows lead from central nervous system to the muscles in several ways, some of them have the feedback mechanism. Human locomotion has only recently begun to understand through the application of nonlinear data processing techniques to study stride interval data. It has been known for over a century that there is variation of 3-4 % in the stride intervals of human during walking but only in the last few years has been demonstrated that the stride-interval time series exhibits long-time correlation, suggesting that the phenomenon of walking is a self-similar, fractal activity.

When the little children begin to walk, their locomotor system is not fully mature. Our first aim is to characterize the development of mature gait and to compare it with the gait of adult people.

The neurodegenerative diseases are consequence of the interruption of the information flow between the central nervous system and muscles. Our second aim is to search the difference of the dynamics between people with neurodegenerative diseases and healthy controls. In the concrete we are studying people with amyotrophic lateral sclerosis, Huntington’s disease and Parkinson’s disease. We are using visual recurrence analysis. We want to consider if this method could help in diagnosis of these diseases.

1. HUMAN LOCOMOTION AND THE NEURODEGENERATIVE DISEASE

1.1. Locomotion

Locomotion is one of the attributes of the life. It is necessary to obtain food, to escape before enemy, between people to make a work, communication and other social functions.

Locomotion and posture of the body are high organised functions, on which muscels, receptors, vegetative nervs and almost all parts of the central nervous system participated. Locomotion can be divided into voluntary and involuntary motion. The scheme of the motor control of nervous system is on the Figure 1.1 [Trojan et al., Fyziologia 2]:

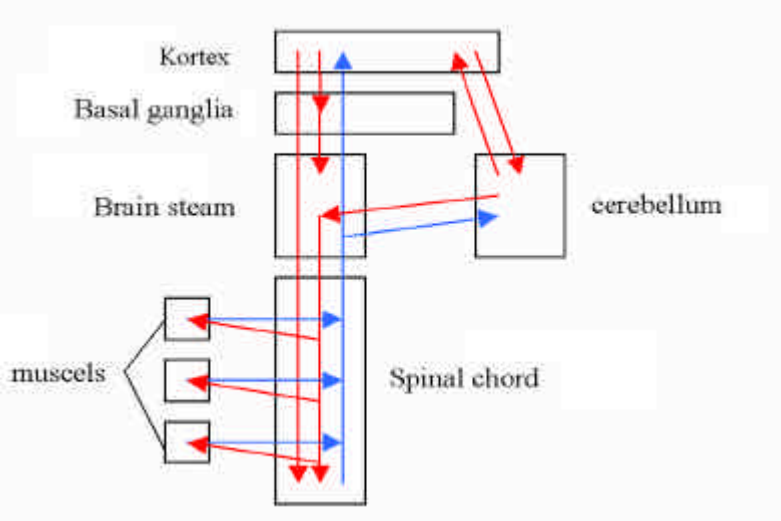

Figure 1.1.

Nervous system is structurally and functionally arranged. The basist reflexes are controled by the spinal chord. Through the dorsal root the spinal chord receives information from sensory perception and the ventral horns contain the α-motor neurons, whose travel through the ventral root direct to the muscles.

The more difficult reflexes are analysing in the upper parts of the central nervous system and the outgoing informations are then sending with pyramidal and extrapyramidal tracts to the spinal chord. Pyramidal tracts connect direct the motor cortex with the motor neurons in the spinal chord. There is a system of feedbacks through the reticular formation, cerebellum, and basal ganglia. Pyramidal tracts provide

the informations about the impuls of the voluntary motion, they drive the fast and exact locomotions. Extrapyramidal tracts carry forward the information from the cortex through the basal ganglia, thalamus, motor centres of the midbrain, pont and the reticular formation to the spinal chord. This system assures slow and difficult locomotion, it is also importent for the coordination of voluntary and involuntary motion. Very importent parts are basal ganglia and cerebellum. The output of the cerebullum is excitatory, while the basal ganglia are inhibitory. The balance between these two systems enables the smooth and coordinated movements.

1.2. Neurodegenerative diseases

Neurodegenerative diseases are a group of disorders characterized by changes in the normal neuronal function, leading, in most cases, to neuronal death. They are sometimes referred to as "system degenerations" as they tend to affect selectively certain specific system of the nervous system. In most instances, the etiological causes are unknown and they have a progressive development.

Neurodegenerative diseases can be divided:

- Diseases affecting predominantly the cerebral cortex (Alzheimer’s disease, Pick’s disease, Creutzfeld-Jakob disease)
- Diseases affecting predominantly the basal ganglia (Parkinson’s disease, Huntington’s disease)
- Spino-cerebellar degeneration (Friedreich's ataxia, Olivo-ponto-cerebellar atrophy)
- Motor neuron diseases (amyotrophic lateral sclerosis)

1.2.1. Amyotrophic lateral sclerosis (ALS)

ALS was first described in scientific literature in 1869 by the French neurologist Jean-Martin Charcot. The term ALS comes from Greek words: a - without, myo - muscle, trophic - nourishment, lateral - side, sclerosis - hardening or scarring.

ALS is a fatal neuromuscular disease, which induces the gradual degeneration and death of the motor neurons. The flow of information between the central nervous system and muscles is broken and the brain looses the ability to start and control the

voluntary movements. When an ALS patient first notices neurological symptoms, more than half of the motor neurons may already be dead. ALS destructs only motor neuron, so mental functions maintain intact.

ALS symptoms may include tripping, stumbling and falling, loss of muscle control and strength in hands and arms, difficulty speaking, swallowing and/or breathing, chronic fatigue, and muscle twitching and/or cramping. ALS is characterized by both upper and lower motor neuron damage. Symptoms of upper motor neuron damage include stiffness (spasticity), muscle twitching (fasciculations), and muscle shaking (clonus). Symptoms of lower motor neuron damage include muscle weakness and muscle shrinking (atrophy). Most ALS patients first notice muscle weakness in either the arms or the legs (32 percent in the arms and 36 percent in the legs.) This is called limb-onset ALS.

Approximately 25% of ALS patients have difficulty speaking as their first symptom. This is called bulbar ALS because it involves the corticobulbar area of the brainstem. ALS is a very variable disease, and there are also cases affecting breathing first, without any other symptoms. Approximately 7 percent have difficulty breathing (dyspnea) as their first symptom.

The cause of ALS is unknown and also we do not have an efficient cure, only some medications whose help to relieve the symptoms. Therapies, supplements, and proper nutrition can be part of a treatment plan. The incidence of ALS is two persons pro 100.000 people. Men get ALS more than women (the ratio is 1.5 to 1.0). 80% of ALS cases begin between the ages of 40 to 70. At least 10% of ALS cases are hereditary. This is called familial ALS. Generally, we define familial ALS as two or more cases in the same bloodline. In familial ALS the disease is autosomal dominant, meaning that if a parent has ALS, their children have a 50% chance of inheriting the defective gene.

50% of ALS patients die within 18 months after diagnosis. Only 20% survive 5 years and 10% live longer than 10 years. Persons with ALS who go on a ventilator may live for many years. Improved treatment is allowing ALS patients to live longer than before. A common cause of death among ALS patients is respiratory failure or cardiac arrhythmias due to insufficient oxygen. Another common cause of death is respiratory infection such as pneumonia. The risk of respiratory infections increases as weakened diaphragm and chest muscles make it more difficult to clear the lungs.

1.2.2. Huntington's disease (HD)

HD is a dominant hereditary illness, it was first described in the year 1872 by George Huntington. HD typically begins in mid-life, between the ages of 30 and 45, athough there are some cases when onset occured about the age of 2. Children who develop the juvenile form of the disease rarely live to adulthood. Each child of a person with HD has a 50% chance of inheriting the fatal gene. Everyone who carries the gene will develop the disease. In 1993, the HD gene was isolated and a direct genetic test developed which can accurately determine whether a person carries the HD gene. The test cannot predict when symptoms will begin.

Early symptoms of HD may affect cognitive ability or mobility and include depression, mood swings, forgetfulness, clumsiness, involuntary twitching and lack of coordination. As the disease progresses, concentration and short-term memory diminish and involuntary movements of the head, trunk and limbs increase. Walking, speaking and swallowing abilities deteriorate. Eventually the person is unable to care for him or herself. Death follows from complications such as choking, infection or heart failure.

At this time, there is no way to stop or reverse the course of HD. Physicians prescribe a number of medications to help control emotional and movement problems associated with HD. Most drugs used to treat the symptoms of HD have side effects such as fatigue, restlessness, or hyperexcitability. It is extremely important for people with HD to maintain physical fitness as much as possible, as individuals who exercise and keep active tend to do better than those who do not.

1.2.3. Parkinson disease (PD)

Parkinson's disease was first described in 1817 by James Parkinson. It is the second most common movement disorder. About 1-2 % of population is affected. Parkinson's disease strikes men and women in almost equal numbers. PD is a disease of late middle age, usually affecting people over the age of 50. The average age of onset is 60 years, only at 5 to 10 % of patients are under 40.

PD results of the lack of dopamine-producing nerve cells. Dopamine is a neurotransmitter, which facilitates the flow of impulses between two parts of the basal

ganglia - from substantia nigra to striatum. The loss of dopamine causes that people are unable to control their movement in normal manner.

Early symptoms of Parkinson's disease are subtle and occur gradually. Patients may be tired or notice a general malaise. Some may feel a little shaky or have difficulty getting out of a chair. They may notice that they speak too softly or that their handwriting looks cramped and spidery. They may lose track of a word or thought, or they may feel irritable or depressed for no apparent reason. This very early period may last a long time before the more classic and obvious symptoms appear.

The four primary symptoms of PD are tremor or trembling in hands, arms, legs, jaw, and face; rigidity or stiffness of the limbs and trunk; bradykinesia or slowness of movement; and postural instability or impaired balance and coordination. As these symptoms become more pronounced, patients may have difficulty walking, talking, or completing other simple tasks. The disease is both chronic, meaning it persists over a long period of time, and progressive, meaning its symptoms grow worse over time.

There are various other symptoms whose accompany PD: depression, emotional changes, memory loss and slow thinking, difficult swallowing and chewing or speech changes and sleep problems.

At present, there is no cure for Parkinson's disease. But a variety of medications provide dramatic relief from the symptoms.

2. Nonlinear techniques of time series analysis

The most direct link between chaos theory and the real world is the analysis of time series data in terms of nonlinear dynamics. Most of the fundamental properties of nonlinear dynamical systems have by now been observed in the laboratory. Evidence for chaotic behavior in field measurements has been claimed in many areas of science, including biology, physiology, and medicine, geo- and astrophysics, as well as the social sciences and finance.

2.1. Dynamical systems

When we are analyzing an irregular sequence of measurements, an immediate question is what kind of process can generate such a series. There exist two opposite approaches - nonlinear deterministic and linear stochastic ones.

In the deterministic picture, irregularity can be autonomously generated by the nonlinearity of the intrinsic dynamics. Let the possible states of a system be represented by points in a finite dimensional phase space - R^d. The transition from the system's state x (t_1) at time t_1 to its state at time t_2 is then governed by a deterministic rule: $x(t_2) = T_{t_2 - t_1}(x(t_1))$. This can be realized either in continuous time by a set of ordinary differential equations:

$$\dot{x}(t) = F(x(t)) \qquad (2.1)$$

or in discrete time t = nΔt by a map of R^d onto itself:

$$x_{n+1} = f(x_n) \qquad (2.2)$$

The family of transition rules T_t, or its realisation in the forms (2.1) or (2.2), are referred to as a dynamical system. The particular choice of F (resp. f) allows for many types of solutions, ranging from fixed points and limit cycles to irregular behaviour.

If the dynamics is dissipative the points visited by the system after transient behaviour has died out will be concentrated on a subset of Lebesgue measure zero of phase space. This set is referred to as an attractor, the set of points that are mapped onto it for $t \to \infty$ as its basin of attraction. Since not all points on an attractor are visited with the same frequency, one defines a measure μ(x)dx, the average fraction of time a typical trajectory spends in the phase space element dx. In an ergodic system, μ(x) is the same for almost all initial conditions. Phase space averages taken with respect to μ(x)dx are then equal to time averages taken over a typical trajectory.

In real world systems, pure determinism is rather unlikely to be realised since all systems somehow interact with their surroundings. Thus the deterministic picture should be regarded only as a limiting case of a more general framework involving fluctuations in the environment and in the system itself. However, it is the limiting case that is best studied theoretically and that is expected to show the clearest signatures in observations.

The opposite approach to analysis of the time series is that external random influences causing the irregularity, while only linear rule may be sufficient to explain the structure in the sequence. The most general linear model is the autoregressive moving average process, giving by:

$$x_n = \sum_{i=1}^{M} a_i x_{n-i} + \sum_{i=0}^{N} b_i h_{n-i} \qquad (2.3)$$

where $\{\eta_n\}$ are Gaussian uncorrelated random increments.

2.2. Phace space and embedding

The time evolution is given by a dynamical system in phase space. Since usually the state points can not be observed directly but only through a measurement function, typically involving a projection onto fewer variables than phase space dimensions, we have to recover the missing information in some way. This can be done by time delay embeddings and related methods. We can then quantify properties of the system through measurements made on the embedded time series. Since it is eventually the underlying system we want to characterise, these properties should ideally be unaffected by the measurement and the embedding procedure. The theoretical framework of this approach is set by a number of theorems, all of which specify the precise conditions when an attractor in delay coordinate space is equivalent to the original attractor of a dynamical system in phase space.

Let {x(t)} be a trajectory of a dynamical system in R^d and {s(t) = s(x(t))} the result of a scalar measurement on it. Then a delay reconstruction with delay time τ and embedding dimension m is given by

$$\vec{s}(t) = (s(t-(m-1)t), s(t-(m-2)t),..., s(t)) \qquad (2.4)$$

The delay embedding theorem by Takens [Takens, 1981] states that among all delay maps of dimension m = 2d+1, those that form an embedding of a compact manifold with dimension d are dense, provided that the measurement function $s : R^d \rightarrow R$ is C^2 and that either the dynamics or the measurement function is generic in the sense that it couples all degrees of freedom. In the original version by Takens, d is the integer dimension of a smooth manifold, the phase space containing the attractor. Thus d can be much larger than the attractor dimension.

2.3. Lyapunov exponents

The hallmark of deterministic chaos is the sensitive dependence of future states on the initial conditions. An initial infinitesimal perturbation will typically grow exponentially, the growth rate is called the Lyapunov exponent. Let x_{n1} and x_{n2} be two points in state space with distance $||x_{n1} - x_{n2}|| = \delta_0 << 1$. Denote by $\delta_{\Delta n}$ the distance after a time Δn between the two trajectories emerging from these points,
$\delta_{\Delta n} = ||x_{n1+\Delta n} - x_{n2+\Delta n}||$ then the Lyapunov exponent λ is determined by

$$\delta_{\Delta n} \cong \delta_0 e^{\lambda \Delta n}, \quad \delta_{\Delta n} << 1, \quad \Delta n >> 1. \qquad (2.5)$$

A positive, finite value of λ means an exponential divergence of nearby trajectories, which defines chaos. Here, only the single (maximal) Lyapunov exponent will be discussed. Lyapunov spectra can be defined that take into account the different growth rates in different local directions of phase space. However, the non-leading exponents are notoriously difficult to estimate from time series data. Only in very few cases of clean laboratory time series trustworthy results have been obtained so. For field data, Lyapunov spectra beyond the first exponent have not so far been demonstrated to be a useful concept.

There have been a number of attempts to generalise the Lyapunov exponent to systems which are not purely deterministic. For the usual definition, an arbitrarily small amount of noise leads to a diffusive separation of initially close trajectories and a divergent Lyapunov exponent (mind the order of the two limits involved). For very small noise levels, there may still be a range of length scales where the separation proceeds exponentially, until the finite size saturation is reached. This is the behaviour that is probed by the real space methods of estimating Lyapunov exponents from data, in particular the two very similar algorithms introduced independently by Rosenstein et al. [Rosenstein et al., 1993], and by Kantz [Kantz, 1994]. From the theoretical point of view, intermediate length scale definitions are less attractive since the resulting quantities are no longer invariant under smooth coordinate transformations. An alternative way to introduce noise into the definition of Lyapunov exponents is to study the separation of initially close trajectories of two identical copies of a system that are evolving subject to the same noise realisation. Then the Lyapunov exponent quantifies the contribution to the divergence that originates in the intrinsic instability of the

deterministic part of the system. This is essentially the kind of instability probed by the tangent space methods to obtain Lyapunov exponents from data.

2.4. Linear observable

In the linear approach to time series analysis, a quantitative characterisation of a process is done on the basis of either the two-point autocovariance function or the power spectrum. If only a finite time series $\{s_n, n = 1 . . .N\}$ is available, the autocovariance function can be estimated by:

$$C(t) = 1/(N-t) \sum_{n=t+1}^{N} s_n s_{n-t} \qquad (2.6)$$

Depending on the circumstances, other estimators may be preferable. A whole branch of research is devoted to the proper estimation of the power spectrum from a time series. The simplest estimator, known as the periodogram Pk, is based on the Fourier transform of $\{s_n\}$,

$$S_k = \sum_{n=0}^{N-1} s_n e^{i2pkn/N} \qquad (2.7)$$

through $P_k = |S_k|^2$. According to the Wiener-Khinchin theorem, the power spectrum of a process equals the Fourier transform of its autocovariance function. For finite time series this is only true if either $C(\tau)$ is computed on a periodically continued version of $\{s_n\}$, or Pk is computed on a version of $\{s_n\}$ that is extended to n = -N, . . . ,N by padding with N zeroes. Nevertheless, both descriptions contain basically the same information, only that it is presented in different forms.

The power spectrum of a process is unchanged by the time evolution of the system (if it is stationary). However, it is affected by smooth coordinate changes, e.g. by the characteristics of a measurement device. Usually, the non-invariance of the power spectrum is not a serious drawback. The power spectrum is most useful for the study of oscillatory signals with sharp frequency peaks. The location of these peaks is conserved, only their relative magnitude may be affected by the change of coordinates. Sharp peaks in the power spectrum indicate oscillatory behaviour and are useful indicators in linear as well as in nonlinear signals. Broad band contributions, however, have a less clear

interpretation since they can be either due to deterministic or stochastic irregularity. Therefore, the power spectrum is only of limited use for the study of signals with possible nonlinear deterministic structure.

2.5. Dimension and entropy

The chaotic dynamical systems are characterized besides the exponentially divergence of the trajectories by the irregular geometry of the sets in phase space visited by the system state point in the course of time. The divergence of the trajectories can be realized in a finite phase space only through some folding mechanism. Stretching, folding and volume contraction lead to statistically self-similar structure on small length scales. The loss of information due to the folding is reflected by the entropy of the process.

The self-similar structure can be characterized by the fractal dimension. Most well known is the Hausdorff dimension of the set and more easily computable box counting dimension. We can also weight the points in the set by the frequency with which they are visited on average, then we need a definition of the dimension in terms of the natural measure μ(x)dx. It could be defined by means of correlation integrals $C_q(e)$. Let ?(x) be the locally averaged density:

$$r_e(x) = \int_y dym(y)\Theta_e(1 - \| x - y \| / e) \qquad (2.8)$$

where $T_e(1\text{-}r/e)$ is the Heaviside step function, T(x) = 0 if x = 0, T(x) = 1 for x > 0. The correlation integral of the order q is given:

$$C_q(e) = \int_x dxh(x)[r_e(x)]^{q-1} \qquad (2.9)$$

For a self-similar process we have:

$$C_q(e) \approx e^{(q-1)D_q}, e \to 0 \qquad (2.10)$$

D_q is called the order-q dimension. D_0 has been shown to coincide with the Hausdorff dimension. D_1 is the information dimension – it quantifies the scaling of the amount of information needed to specify the state of the system with the required accuracy. D_2 is the correlation dimension – a means of quantifying the “strangeness” of an atractor [Grassberger,Procaccia, 1983].

When analysing time series we are usually dealing with distributions of delay vectors with delay t in an m-dimensional reconstructed phase space. The m dependence of C_q in the limit of large m can be expressed as:

$$C_q(m,e) = a(m)e^{-(q-1)h_q mt} e^{(q-1)D_q}, e \to o, m \to \infty \qquad (2.11)$$

which defines the order q entropy h_q. The prefactor a(m) depends on the norm.

2.6. Nonlinear analysis of limited data

Real word data are represented with a finite length and noise time series so the previous definitions and concepts have to be adapted to this conditions. The way to proceeds crucially depends on the point of view we want to assume about the nature of the system. We can not assume the deterministic chaos for any time series, we have to establish it from the data. But we may still borrow some concepts just because they give a convenient framework for certain problems.

The embedding theorem assumes that the observations are available with arbitrary precision and arbitrarily small length scales can be accessed, which implies that an infinite amount of information is available. Several authors have investigated what happens to the embedding procedure when noise is present and the sequence is of finite length.

For the embedding procedure noise is the dominant limiting factor. First we need to make a distinction between noise due to measurement error, then a deterministic dynamical system is underlying the signal, and noise that is intrinsic to the dynamical system. If the noise is coupled to the system we have to specify in what sense we want to use the embedding in the first place. The nature of the noise is usually not known independently. There is no general way to infer its properties from time series without making strong assumptions about the dynamical system or the spectral properties of the noise.

One study about the effect of measurement noise on the embedding procedure is that by Casdagli and coworkers [Casdagli et al., 1991]. Their main result is that a reconstruction technique that leads to a formally valid embedding with noise free data can nevertheless amplify the noise even in a singular way. That means that in such a case not all degrees of freedom of the system can be recovered from a scalar time series even for arbitrarily small amount of noise.

There are some results on the embedding of noise driven signals. One line of though supposes that the driving noise sequence is known. The dynamical system then becomes a nonlinear input-output device. The observation of the output of such a system can be embedded in the sense that time delayed copies of the observation sequence together with the state of the input variable specify the state of the equally well as the full output together with the input state.

There are other works that also follow the idea that the dynamical noise can be isolated in certain cases where the observations contain sufficient redundancy [Muldoon et al., 1997]. If there are more probes available than necessary to cover the degrees of freedom of the system it's possible to make distinction between the deterministic parts of the signal and the dynamical noise. This allows to recover missing variables by an embedding procedure.

One immediate restriction of the embedding theorem for finite data is that the information contained in a time delay representation is influenced by the choice of embeddings parameters. While embedding theorem do not restrict the delay time t, the proper choice of t does matter for practical applications. Also, there are many cases where the theoretically sufficient embedding dimension m is not optimal for a certain purpose. Larger (but sometimes also smaller) dimension may give better results.

2.7. Estimating dynamics and predicting

An irregular signal can be generated by a nonlinear dynamical system with only a few degrees of freedom. One of the goals should be to find the equations of motion that follow this principle and are consistent with the data. The ability to produce a time series that is equivalent to the measured one can be taken as an evidence for the validity of the approach. If we reconstruct the equations of the dynamical system we are often interested in prediction of future values. Moreover, in many situations the average error when predicting a time series can br taken as a indicator of the structure present in the data.

Chaotic dynamical systems are structural instable. This means that models with very similar parameters may exhibit qualitatively different global dynamics. Therefore, if we simply iterate fitted model equations, we may see substantially different behavior from the actual system even if the model in itself is faithful. One way to moderate this danger is to introduce a small amount of dynamical noise comparable to the modeling

error when iterating the equations. Dynamical noise softens the sensitive dependence on parameters to some extent. Alternatively one could study ensembles of models, which are compatible with the data.

The task is to estimating the function F or f that is supposed to generate the data after the equation (1) or (2) respectively. All we have is a scalar noise time series:

$$s_n = s(x_n) + x_n, \qquad x_n = f(x_{n-1}) + h_n \tag{2.12}$$

Also an intrinsic noise term ? is included because no real system is ever really isolated. Since we cannot completely recover $\{\mathbf{x}_n\}$ from $\{s_n\}$, the best we can do is to use some kind of embedding of $\{s_n\}$ and look for a mapping f_s that acts on the embedding vectors. The standard approach is to choose some parameters dependent model for f_s and optimize the parameters using a maximum likelihood or least squares procedure. This assumes that the value $y = f_s(x)$ is known at a number of locations, with some uncertainty.

As for the model class from which **f** is to be determined, a number of different propositions have been made. One possibility is to expand the dynamics in Taylor series locally in phase space [Eckmann et al. B, 1986]. In practice, the expansion is carried out up to at most linear order. Since one has to work in several dimensions, the number of coefficients in higher order approximations becomes too large for a local treatment. In m-dimensional delay coordinates, the local model is then quite simply:

$$s_{n+\Delta n} = a_0^{(n)} + \sum_{j=1}^{m} a_j^{(n)} s_{n-(j-1)t} \ , \tag{2.13}$$

where ? n is the time over predictions are being made and t is the time delay as usual.

The coefficients $a_j^{(n)}, j = 0,...,m$ may be determined by a least squares procedure, involving only points s_k within a small neighborhood around the reference points s_n . Thus, the coefficients will vary throughout phase space. The fit procedure amounts to solving m+1 linear equations for m+1 unknowns.

The optimal degree of locality of a locally linear modeling approach has been used as a measure for nonlinearity in a time series. It is compared the predictive quality of models fitted with using different numbers of neighbors. In the absence of nonlinearity, the globally linear fit using all available points as neighbors should give best results since it uses the largest number of points and is structurally more robust. For increasing degrees of nonlinearity, the tradeoff between lack of statistics with few

neighbors and curvature error with large neighborhoods should move the optimum towards smaller length scales. So we can estimate the degree of nonlinearity what is the most useful assumption for modeling.

The different class of approaches for modeling attempts to fit the dynamics by a nonlinear function that is globally defined in the phase space. So the task is to minimize this expression:

$$\sigma^2 = \sum_n (s_{n+1} - \mathbf{f}_p(s_n))^2 \qquad (2.14)$$

where $\mathbf{f}_p$ is now a nonlinear function with parameters p, with respect to which the minimization is done. Polynomials, radial basis functions orthogonal polynomials and others functions have been used.

2.8. Nonstationarity and Recurrence Plots

Almost all methods of time series require some kind of stationarity. Therefore, changes in dynamics during the measurement are undesirable. But sometimes these changes represent the most interest information about the system. In the past the question was solved how to established the stationarity. If nonstationarity was detected, often time series was discarded as unsuitable for detailed analysis, or it was split into segments that were short enough to be regarded as stationary. More recently, authors have begun to recover the information contained in time-variable dynamics as an essential part of the underlying process.

The most common definition of a stationary process is that all conditional probabilities are constant in time. This definition is not applicably for real world processes. If we regard deterministic process a limiting case of stochastic process where the conditional probability density for a transition from the state x to x' is given by $d(x' - f(x))$, the definition requires $f()$ to be unchanged. The transition probabilities are unknown and have to be estimated from the data, subject to statistical fluctuations. In some cases these fluctuations are large and the properties of measured data can changed dramatically, even though the underlying process is formally stationary after the above definition. There is no agreement on a definition of a stationary process. It is reasonable to require that the duration of the measurement is long compared to the time

scales of the system. Then all temporal changes can be modeled as part of the dynamics. So processes with power low correlations are often considered nonstationary since no length of measurement could ever cover all time scales. On the other hand, processes with very well separated time scales can lead to time series which are stationary for practical purposes.

There are a lot of statistical tests for nonstationarity. Most of them is based on estimating a parameter by using different parts of time series. If variations are found to be significant, the time series is regarded as nonstationary.

When thinking of geometry in the phase space, nonstationarity introduces a tendency that points close in space are also close in time. The basic graphical tool that evaluates temporal and space distance of states is recurrence plot of Eckmann [Eckmann et al., 1987]. Recurrence Plots (RPs) are relatively new technique for the qualitative assessment of time series. With RP, one can graphically detect hidden patterns and structural changes in data or see similarities in patterns across the time series under study.

Recurrence plots are intricate and visually appealing. They are useful for finding hidden correlations in highly complicated data. Because they make no demands on the stationarity of a data set, RPs are particularly useful in the analysis of systems whose dynamics may be changing. The use of recurrence plots in time-series analysis has become more common in recent years, particularly in the area of physiology.

An RP is a two-dimensional representation of a single trajectory. The time series spans both ordinate and abscissa and each point (i, j) on the plane is shaded according to the distance between the two corresponding trajectory points y_i and y_j. In an unthresholded RP (UTRP) the pixel lying at (i, j) is color-coded according to the distance, while in a thresholded RP (TRP) the pixel lying at (i, j) is black if the distance falls within a specified threshold corridor and white otherwise. RPs are symmetrical along the x = y axis, where each point is plotted against itself and this diagonal roughly represents time [Zbilut, Webber, 1992]. The RP generated from a chaotic data set is far more complicated, although it too has block-like structures resembling to what might be expected from a periodic signal. For random signal, the uniform (even) distribution of colors over the entire RP is expected and the colors on the UTRP for the time sequence "deepen" away from the main diagonal.

The basic idea behind the interpretation of the RPs is simple: if the underlying signal is truly random and has no structure, the distribution of colors over the RP will be

uniform, and so there will not be any identifiable patterns. If, on the other hand, there is some determinism in the signal generator, it can be detected by some characteristic, distinct distribution of colors. The main advantage of the recurrence plots over another widely used techniques as for example Fourier analysis, is that they preserve both temporal and spatial dependence in the time series. Even though Fourier analysis reveals the distribution of spectral frequencies, it does not show how self-similar, resonant frequencies are patterned as a function of time. Yet, RP is mostly a qualitative tool and the precise meaning of the patterns is unknown.

3. Present State of Human Locomotion Analysis

3.1. Measures of Stride-to-Stride Variability

The basis means to estimate the stride-to-stride variability is the standard deviation (SD) and the coefficient of variation (CV = 100 * SD / mean). But these measures can not distinguish between gait with large stride-to-stride variations and gait with small variations from one stride to the next one, but influenced with long-range changes, for example with the change in speed. To eliminate the local changes in the mean SD of the first difference of the time series is calculated.

3.2. Measurements of the Temporal Structure

Spectral analysis

Fourier spectral analysis is one of the standard methods for studying the dynamics of the time series. To remove the effects of the length, mean and SD of the time series, the same number of strides is taken into account, from each value is subtracting the mean and it is dividing by the SD. This produces a time series with mean 0 and with SD equals to 1.0. Then the standard Fourier transformation is performed, with the use of a rectangular window. The ratio of the percentage of power in the low frequency band to percentage of power in the high frequency band determines the "balance" of the spectra. The large ratio indicates nonstationarity.

To quantify the dynamic differences in time series we can calculated the ß exponent, which is the negative slope of the regression line drawn through the double log graph of power versus frequency. A ß-exponent of 0 represents the white noise, whereas others values suggest that there are correlations in the data. A value close to 1 reveals the long-range, fractal correlations, the value 2 indicates the Brownian noise also known as the random walk.

Autocorrelation decay

Autocorrelation function has the information about the "memory" of the system. It estimates how the time series is correlated with itself over different time lags: Two indexes are calculated τ_{37} and τ_{67}. τ_{37} (τ_{67}) is equals the number of the strides, after whose the autocorrelation function decays to 37 % (67%) of its initial value.

Detrended fluctuation analysis (DFA)

DFA is method, which studies the long-range, fractal properties in long time series or how change the correlation relations over different time scales. Self-similarity and the fractional dimension characterize fractal objects. Self-similarity means that there exist subsets whose after proper scaling have the same statistical properties as the whole set.

First is the time series is integrated:

$$y(k) = \sum_{j=1}^{k} [x(j) - x_{ave}] \qquad (3.1)$$

where x(j) is j-st point in the time series of length N and x_{ave} is the average value of the time series.

Next the integrated time series is divided into boxes wit same length n, in each box the least-square line fitting $y_n(k)$ is calculated. The integrated time series is detrended by subtracting the local trend $y_n(k)$ and the root-mean square fluctuation F(n) is calculated:

$$F(n) = [(1/N)\sum_{k=1}^{N} [y(k) - y_n(k)]^2]^{1/2} \qquad (3.2)$$

This computation is repeated for different box sizes to capture relationship between F(n) and the box size n. The slope of the double log-log graph determines the fractal scaling index α.

- For white noise where the values are completely uncorrelated α is equals to 0.5
- For short-term correlation α is differ from 0.5, but it will approach 0.5 for large window sizes.
- An α greater than 0.5 but less than or equal 1.0 indicates long-range power-low correlations
- When $\alpha > 1$, correlations exist but cease to be of a power-low form
- $\alpha = 1.5$ indicates the brown noise
- when $0 < \alpha < 0.5$ power-low anticorrelations are present, large values are more likely to be followed by small values and vice versa

The fractal scaling a is related to ß-exponent by formula: $a = (ß + 1)/2$.

Normalized nonstationarity index (NSI)

NSI is used to evaluate how the local average is change during the process, independent of the fluctuation magnitude. The same number of points of the time series is taken and normalized with respect to the mean and SD. This new time series is divided into segments and local averages are computed. NSI is defined as the SD of these local averages. NSI provides a measure of the consistency of the local average values, independent of the overall variance of the original time series. Higher NSI values indicate more inconsistent local averages.

3.3. Maturation of gait dynamics

When children learn to walk, this activity is accompanied with frequent falls and large stride- to-stride variability. In the age about three years old their gait appears relatively mature. But the neuromuscular control is developed beyond this age, so subtle changes in the gait dynamics are assumed.

In adult healthy people the gait duration is changed too, but with small magnitude of the fluctuations. Although this variability appears random, with no correlation between successive strides, the locomotor system possesses "memory", so the change from one stride to the next one displays temporal structure with fractal organization.

The variability of the stride time decreases in children with age. The typical time series of 4-, 7- and 11-years old children are in the Fig. 3.1.[Hausdorff et al. (A), 1999]:

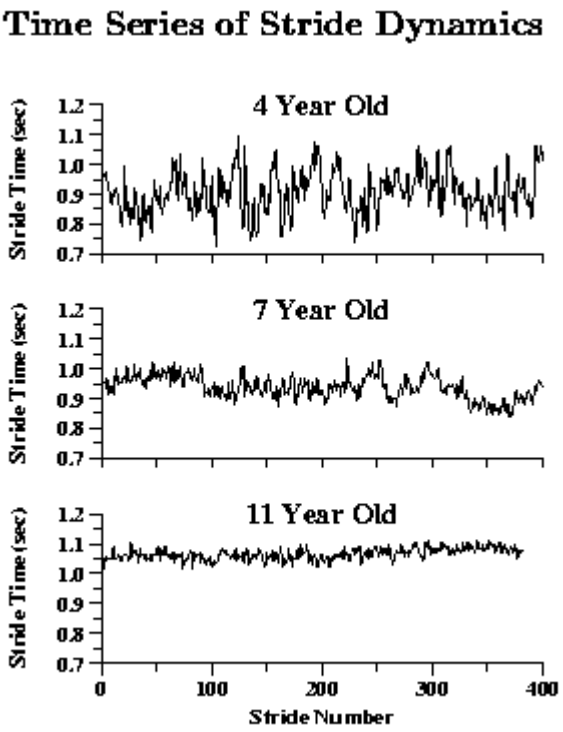

Figure 3.1

Both SD and CV are significantly larger in the 3- years old children than in 6-7 years old children, and this is larger in comparison with 11-14-years old children. The value of SD and CV of 11-14 years old children is very close to the value of young adults. Even after detrending, which can exclude the effect due to fatigue and speed change during the walk, variability is larger in younger children and smaller in older ones.

Also the temporal structure of gait is not fully developed in the children and in the oldest children the stride dynamics approaches the values observed in adults. Different features of the stride dynamics do not develop at the same time.

There is a change in the frequency spectrum with age. The power in the higher frequency band appears to be slightly increasing with age, conversely the power in the lower frequency band is largest in the youngest children. So the low-to-high spectral ratio, the indicator of stability, is larger in the older children and the gait dynamics becomes with age more stable.

Similar results provide autocorrelation measurements. The decay of the autocorrelation function also varied with age. The value τ_{63} rises from 2-3 strides in 3 years old children to 5-6 strides in the 14 years old children, τ_{37} increases from 5-6 strides to 19 ones [Hausdorff et al., 1999].

The fractal scaling index α is similar for the children in the age 3-7 years, its value is $\alpha = 0.93+ 0.03$ and decreases in older children (11-14eyars old) to $0.88 + 0.04$ [Hausdorff et al., 1999]. The mean α of the oldest children was closest to the value obtained in young adults.

In children, gait is over certain age ranges influenced with the body size - the leg length, height. The velocity of gait increases in the age of 6-7 years. Even after adjusting to these factors

The above results are available (the dynamical measurements were normalized with respect to height).

3.4. Analysis of Parkinson's disease, Huntington's disease and Amyotrophic lateral sclerosis

Parkinson's disease (PD), Huntington's disease (HD) and amyotrophic lateral sclerosis (ALS) are neurodegenerative diseases, PD and HD are disorders of the basal ganglia and ALS is motor neuron disease. PD, HD and ALS display some common features of altered stride dynamics, as well as distinct ones.

A representative time series of this disorders and healthy controls are shown on Fig 3.2 [Hausdorff et al., 2000 (C)]:

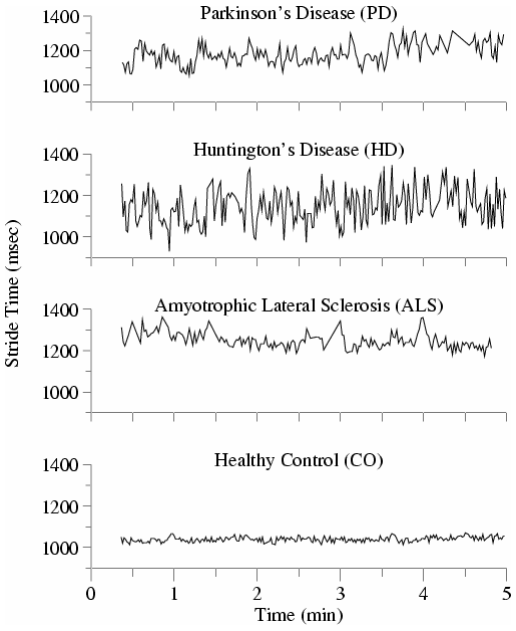

Figure 3.2

One common feature is the less speed of gait. This feature may by a general marker of neurodegenerative diseases, but it is not possible to distinguish among these disorders.

Stride-to-stride variability is increased in all three disorders. The average stride time is much longer for subjects with ALS compared with the control subject an also compared with that of subjects with HD and PD, in subjects with PD is the stride time similar as in control subjects.

The variability of the stride time is larger for all diseases. The value of CV and SD of the detrended time series are about twice as large in ALS and PD subjects compared with control, but in HD subjects this values become yet larger.

All measures of the fluctuation dynamics are most changed in subjects with HD compared with both healthy control and subjects with PD and ALS. Fractal scaling index α and autocorrelation decay time tended to be lower in ALS subjects compared with controls, nonstationarity index is similar. In subjects with PD is fractal scaling index lower than in controls, autocorrelation decay time is slightly larger than in controls and NSI is comparable with NSI of control subjects.

Changes are evident also when studying subjects with mild lower extremity impairment comparing with controls. Subjects with mild form of ALS have increased stride time and decreased autocorrelation decay time. Among HD subjects all measures of fluctuation magnitude and dynamics are significantly different compared with controls, except for NSI for which the difference is marginal. Among PD subjects the measures of fluctuation magnitude are significantly increased.

To evaluate any specifically parameters that characterize the three different diseases subjects with advanced ALS (HD, PD) are compared with the other groups having advanced disorders. Prominent features of advanced ALS are longer stride time and slightly increased NSI. Increased fluctuation magnitude, decreased memory and decreased NSI are markers of advanced HD.

In HD, the degree of impairment is measured by using the total functional capacity (TFC) score of United Huntington's Disease Rating Scale. Most impairment belongs to the value 0, and no impairment is equal to 13. The fractal scaling index α is linearly related to this degree of functional impairment.

RESULTS OBTAINED IN THE THESIS

4. Nonlinear structure of human gait dynamics

4.1. Human gait maturation

4.1.1. Analysis of stride intervals and Fourier spectra

Although our primary aim in this thesis is to understand the dynamical structure of the impaired gait during the neurodegenerative diseases it is of course interesting to analyze first how the gait changes in subjects with varying age. The effect of age on gait maturation has been studied for a long time [Gabell, Nayak, 1984], but essentially only a linear methods of analysis were used.

The human body is build for motion. Forty percent of adult body mass is muscle with proportionally more in the lower extremities. Muscles and bones are motors and levers designed to allow movement in many planes. Muscles are necessary not only for propulsion but also for deceleration and shock absorption. Human locomotion also has idiosyncratic characteristics with unique aspects apparent in every individual. We can identify family and friends by their gaits. However, an individual's gait also varies according to speed, mood, footwear and fatigue. Human locomotion is also affected by changes in development such as physiological processes affecting neuromotor control, growing and maturing body segments, variable rotation of limbs and joints about an axis of motion, and changes in posture. The attainment of locomotor skills is a complicated process dependent upon an intact neuromotor and musculoskeletal system.

Human develops all brain cells they will ever have by 20 weeks of intrauterine life. Interneurons appear and reproduce to interconnect brain cells until about age one. The process of myelination takes several years and is completed in a cephalad to caudal (head to tail). There is much individual variation in the rate of development of neuromotor control. Early neuromotor maturation is manifested by the suppression of primitive reflexes or postural responses can reflect a disorder in the central or peripheral nervous system. Primitive reflexes are naturally present in the newborn and infant younger than 6 months. They are never normally obligatory or persistent; rather, infants move in and out of these patterns are gradually completely suppressed. Postural responses, incorporated naturally into movement and locomotion. The evolution of primitive reflexes and postural responses, also occurs proximal to distal. It takes several years for mature pattern to evolve. Characteristics of a mature gait pattern include a

narrow base of support, smooth movements with minimal oscillations of the center of gravity and reciprocal arm swing.

Most practitioners agree a mature gait is present in normal children by age 5. However, after analyzing 186 normal children, Sutherland et al. [Sutherland et al., 1988] concluded a mature gait pattern is well established in most children by age 3. The criteria they used included duration of single-limbe stance, walking velocity, cadence, step length and ratio of pelvic span to ankle spread. Nonetheless, subtle changes in the development of neuromuscular control and locomotor function continue well beyond age 3.

Walking consists of a sequence of steps. These steps may be partitioned into two phases: a stance phase and swing phase.

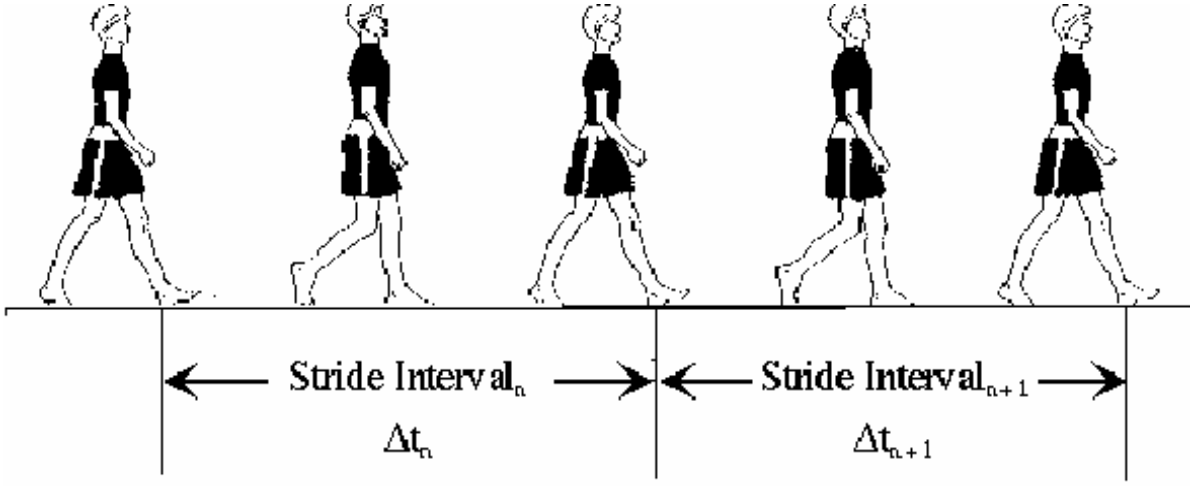

The stance phase is initiated when a foot strikes the ground and ends when it is lifted. The swing phase phase is initiated when the foot is lifted and ends when it strikes the ground again. The time to complete each phase varies with he stepping speed. A stride interval is the length of time from the start of one stance phase to the start of the next stance phase.

Analysis of the stride time dynamics may provide a window into the development of neuromuscular control in children. Given the apparent parallels between the immature gait of children and the unsteady gait of older persons and persons with neurological impairment [Forssberg, Johnels, Steg, 1984], along with the subtle continued development of neural control beyond age 3, the stride time dynamics may not be fully maturated at this age. We have therefore analyzed the development of mature stride dynamics using recurrence quantification analysis to determine at what

ages changes in gait dynamics occurs to compare the gait dynamics of children to those of adults.

The collection of stride intervals were kindly supplied by Dr. Jeff Haussdorf, Harvard Medical School, and were collected by the study of fifty boys and girls with 3-14 years. These subjects walked at their self-determined, normal pace for 8 min around a 400 m running track. All wore their own shoes or sneakers. Representative examples of effects of age on the stride time fluctuations are shown in Fig.1-12.

As can be seen the stride time of the oldest childs is relatively constant throughout the walk. In contrast, for the youngest children the local average appears to change from time to time. Quantitatively this property of gait maturation is shown in Fig. 18a, where the age dependence of mean value of stride intervals is shown. We have further analyzed age dependence of standard deviation (Fig. 18b.), this quantity is largest for the yongest children and decreases with age. Standard deviation characterizes the fluctuation and nonstability of gait, so the gait becomes more stable with age.

Together with a stride intervals we have for all subjects performed fast Fourier transform of time series (Fig.1b.-Fig.12b). We have shown power spectra in the log-log scale, in order to determine the fractal scaling exponent α power ~ $1/f^{\alpha}$, as a slope of linear fit. These values are summarized in the Fig. 17. As can be seen the fractal scaling exponent is largest for oldest subject, and is almost linearly age dependent. The value for the oldest subject is close to the value of fractal scaling exponent for the Brown noise.

4.1.2. Reconstruction of dynamical system behind the stride dynamics

One of the fundamental questions in neuromuscular control research is Bernstein's historical (1935) "degrees of freedom problem": (N. Bernstein, 1935) How are the very many degrees of freedom of the human body coordinated to produce smooth, rational movements ? Human locomotion is known to be a voluntary process, but it is also regulated through a network of neurons called "central pattern generator"(CPG), capable of producing a syncopated output. The early [Bay, Hermani, 1987] nonlinear dynamical models of CPGs for gait assumed that a single nonlinear oscillator has to be used for each limb participating in the locomotion process. Therefore a quadraped required the coupling of four nonlinear oscillators to determine

the correct phase relations among the four legs in order to distinguish between various modes of locomotion, that is , walking trotting, cantering and galloping. More recent dynamical models [Taga, 1996], using the property of synchronization of nonlinear dynamical systems, allows for neurons within an assembly to become enslaved to a single rhythmic muscular activity. Further models assumes that the central nervous system is coupled to the moto-control system, and together they control the locomotion of the gait cycle. According to these studies seems that the global locomotor dynamics is effectively quite low dimensional and, if predominately deterministic, should be expected to be well modeled by e.g. above mentioned dynamical system with a few 1, 4 or 10 state space dimensions. While not specifying precisely how it occurs, these results indicates that human walking involves a substantial “collapse of dimension” from the very high dimensional state space of all possible movements to an approximately 4-10 dimensional subspace.

Our aim is therefore to analyze the correctness of this assumption on the large set of human walking data.

The philosophy behind the theory of dynamical systems is based on the concept that the dynamics of multidimensional system can be recreated and predicted from a single history of anyone of its observable output variables [Takens, 1981]. Using time delayed copies of this observable we can reconstruct the phase space of the dynamical system. Mutual information function can be used to determine the “optimal” value of the time delay for the state space reconstruction, as first proposed in by Fraser and Swinney [Fraser, Swinney, 1986]. The idea is that a good choice for the time delay T is one that, given the state of the system X(t), provides maximum new information with measurement at X(t+T). Mutual information is the answer to the question, "Given a measurement of X(t), how many bits on the average can be predicted about X(t+T)?" A graph of I(T) starts off very high (given a measurement X(t), we know as many bits as possible about X(t+0)=X(t)). As T is increased, I(T) decreases, then usually rises again. It is suggested that the value of time delay where I(T) reaches its first minimum be used for the state space reconstruction.

The “False Nearest Neighbors” (FNN) is a method of choosing the minimum embedding dimension of a one-dimensional time series, suggested by Kennel et al. [Kennel, Brown, Abarbanel, 1992]. This method finds the nearest neighbor of every point in a given dimension, then checks to see if these points are still close neighbors in one higher dimension. The percentage of FNN should drop to zero when the appropriate

embedding dimension has been reached. While the FNN method is intuitive and easy to implement, it is not straightforward to use and interpret. Among some other things, the FNN method requires setting two threshold values to some rather arbitrary values, which are then used to determine the false neighbors. In addition, FNN method is sensitive to the sampling rate of the time series.

For each vector X = (x1, x2, x3, ...xn) in the time series find its nearest neighbor Y = (y1, y2, y3, ..., yn) in an n-dimensional space. Iterate both points and compute R = | x(n+1) - y(n+1) |. This distance R is essentially a distance between the images of vectors X and Y. One may also think of y(n+1) as a predictor for x(n+1), so R is then the prediction error. The idea is that when the attractor is completely unfolded in n dimensions, the distance R between the (n+1)st components of vectors X and Y will be small. To detect if the nearest neighbor just found is false, we compare R (the prediction error) with the errors that would have been made by a trivial predictor. If the error made by the trivial predictor is less than R, we register the nearest neighbor as “false”. The trivial predictor simply uses xn as a predictor x(n+1). So, more formally,

if | x(n+1) - y(n+1) | = | x(n+1) – x(n) |,

the nearest neighbor is labeled as “false”.

We have calculated time delay using AMI method and embedding dimension using FNN method for all 50 subjects. How these quantities depend on the age of subjects is shown in Fig.13-16. Average intrinsic time lag was about 4, and embedding dimension 40. The embedding dimension was calculated also for time delay = 1, but the corresponding embedding dimension was essentially the same. We can therefore conclude that theoretical analysis of a large set of experimental data do not support the idea that there is a substantial “collapse of dimension” and that there is a low-dimensional dynamical system behind the human locomotion as suggested from some previous models or analyses. It should be stressed (see e.g. Fig. 15) that the embedding values are rather scattered (from about 5 to about 60) which mean that the noise of the unknown origin play significant role in the formation of stride interval temporal structure. It is interesting to note that obtained values of embedding dimension are close to the value of 37 corresponding to Brownian motion.

4.1.3. Recurrence quantification analysis

Recurrence plots are extremely useful in visualization of natural time correlation structure of the time series. With RPs we can thus easily locate a wealth of recurring patterns. Moreover we can visualize and detect trends, abrupt changes or drifting dynamics. Recurring patterns appear in the RP as diagonal line segments, parallel to the main diagonal. The representative collection of recurrence plots is shown in Figs. 1.c.-12.c. For comparative purposes we have also calculated randomized (formed by randomly choosing a pair of points from the data chain and exchanging positions of such points, and repeating this procedure N times, where N is the number of all stride intervals) recurrence plots as shown in Figs. 1.d.-12.d. This randomization or shuffling preserves the statistical distribution of the data but changes correlation between points in the data chain and is devoid of coherent phase relationship. For quantitative interpretation of RPs we have for all 50 subjects calculated all standard RQA quantificators as shown in Fig. 17.a.-h. For the quantitative interpretation of these plots we have used recurrence quantification analysis (RQA) method which computes several quantitative variables for each plot, including standard statistics like mean value and standard deviation Other statistics, unique to recurrence plots, are defined: The "*Percent recurrence*" variable quantifies the percentage of the plot covered by recurrent points, and reflects the periodicity in the data. "*Percent determinism*" quantifies the percent of recurrent points that form upward diagonal lines of 4 or more recurrent points, as opposed to being randomly dispersed. "*Line entropy*" addresses the complexity of the RP, in that the more complex the structure of the dynamics of the recurrence plot, the more bits of information are required to describe it, and hence the higher the entropy. "*Max. Line*" is counted as the average of the lengths of diagonal lines and it is the mean prediction time. The inverse of Max. Line is correlated with Lyapunov exponent. The value "*Trend*" is the measure of the fading recurrence points away from the mean diagonal.

When visually inspecting obtained RPs we can see that the distribution of the dots varies for different distances from the main diagonal. From the structure of RPs is clear that the analyzed gait maturation data are mixture of high-dimensional (unknown) deterministic and stochastic (noise) processes. The presence of short lines (destroyed in

the randomized plots, compare Figs. 11.c. and 11.d.) parallel to the main diagonal in some plots mirrors the deterministic character of the system and reflects presence of so-called "unstable periodic orbits", that are embedded in the chaotic attractor of a deterministic system.

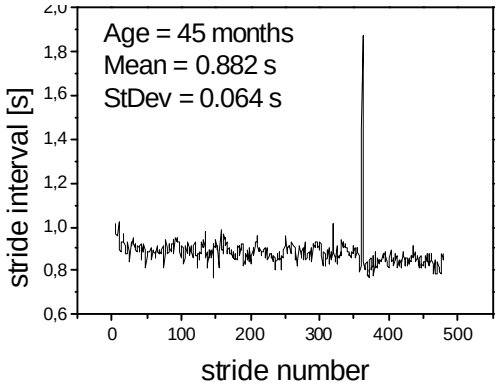

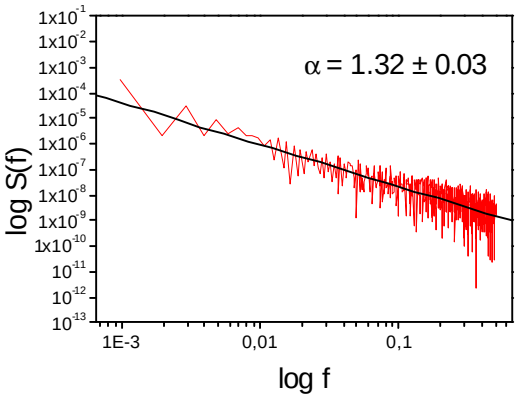

Fig. 1. (a.) Time dependence of stride interval (b.) Power Fourier spectrum of stride intervals

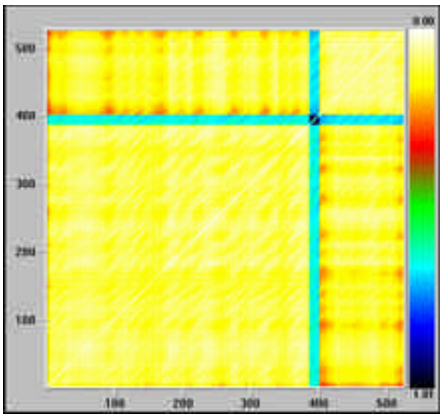

(c.) Recurrence plot of stride intervals

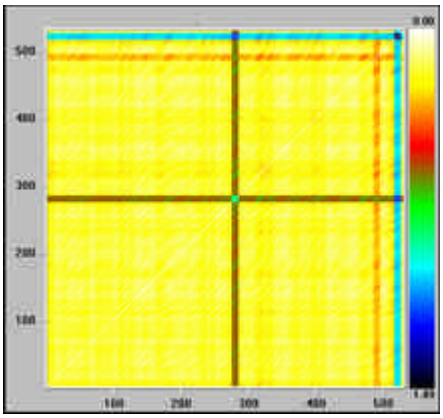

(d.) Randomized recurrence plot

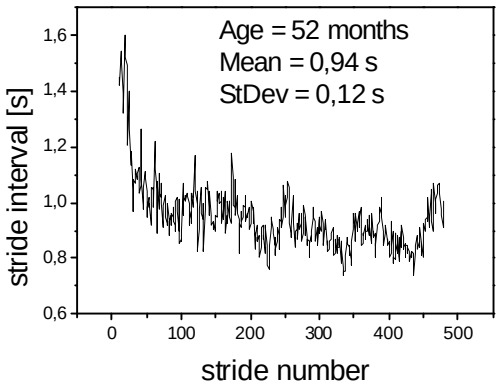

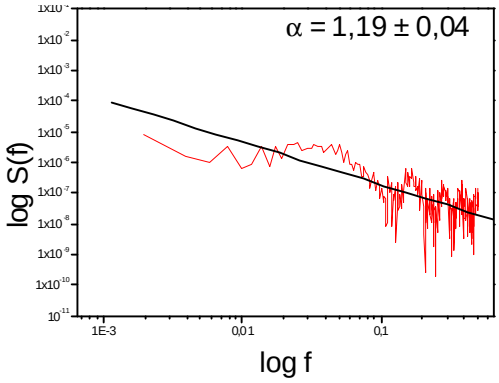

Fig. 2. (a.) Time dependence of stride interval (b.) Power Fourier spectrum of stride intervals

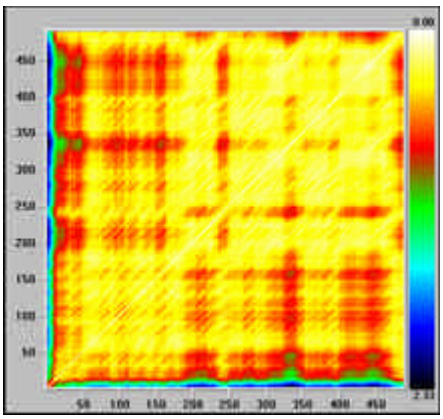

(c.) Recurrence plot of stride intervals

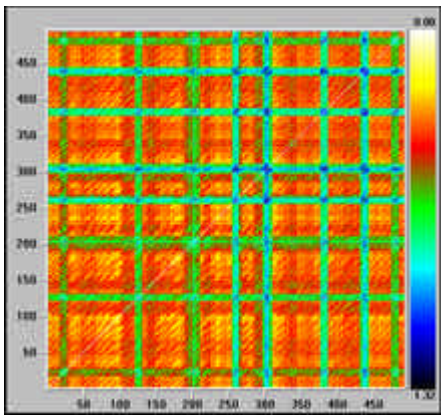

(d.) Randomized recurrence plot

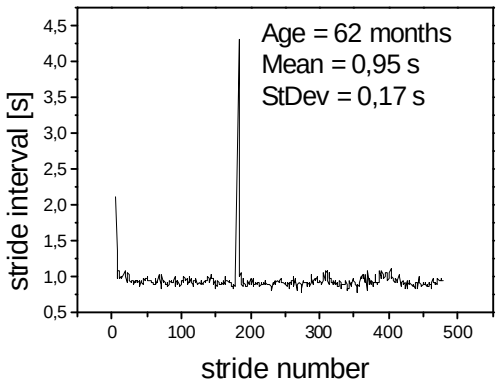

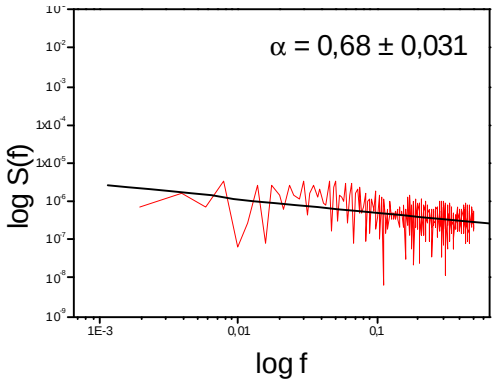

Fig. 3. (a.) Time dependence of stride interval (b.) Power Fourier spectrum of stride intervals

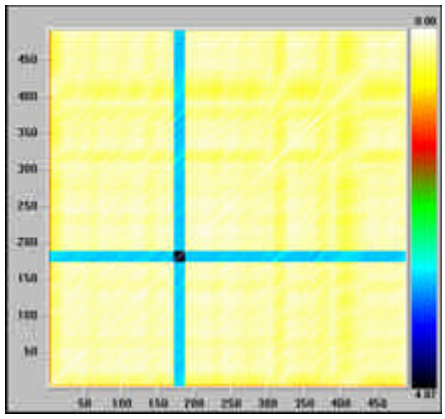

(c.) Recurrence plot of stride intervals

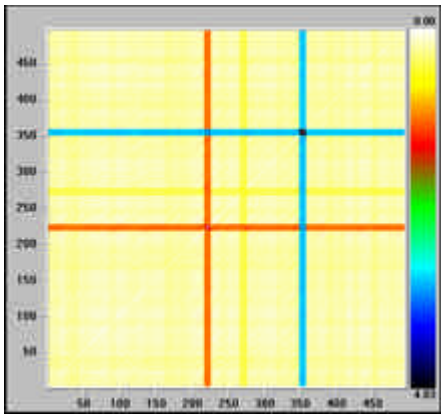

(d.) Randomized recurrence plot

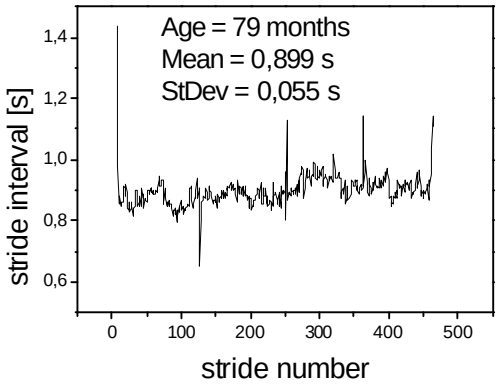

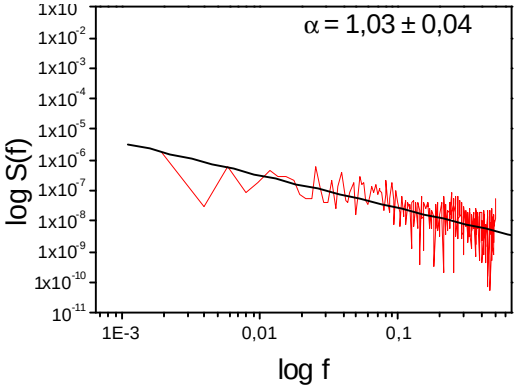

Fig. 4. (a.) Time dependence of stride interval (b.) Power Fourier spectrum of stride intervals

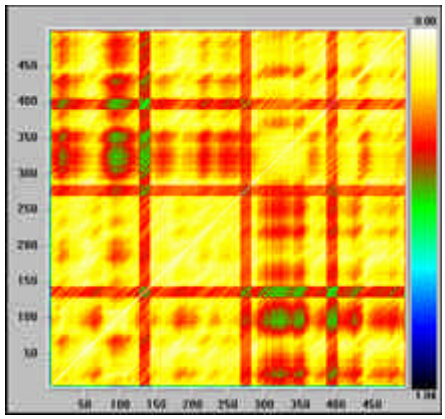

(c.) Recurrence plot of stride intervals

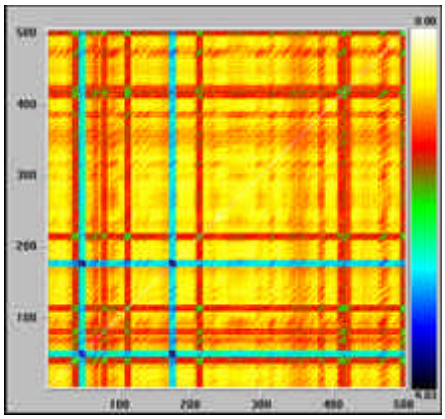

(d.) Randomized recurrence plot

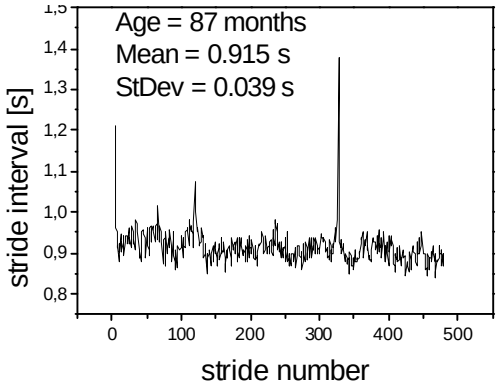

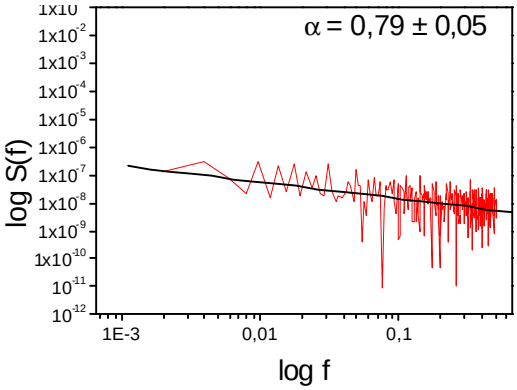

Fig. 5. (a.) Time dependence of stride interval (b.) Power Fourier spectrum of stride intervals

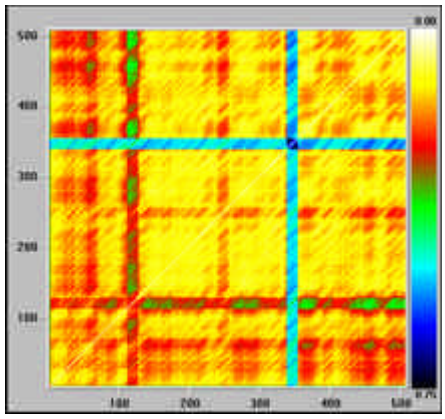

(c.) Recurrence plot of stride intervals

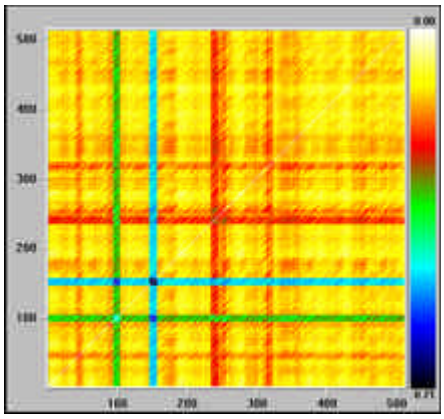

(d.) Randomized recurrence plot

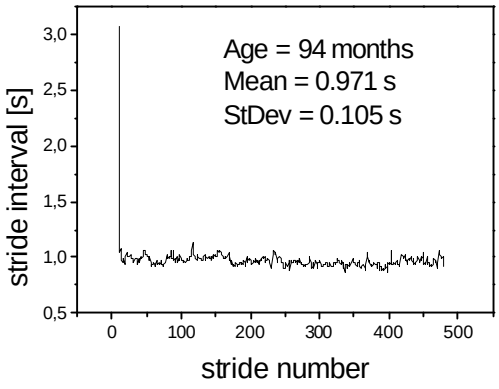

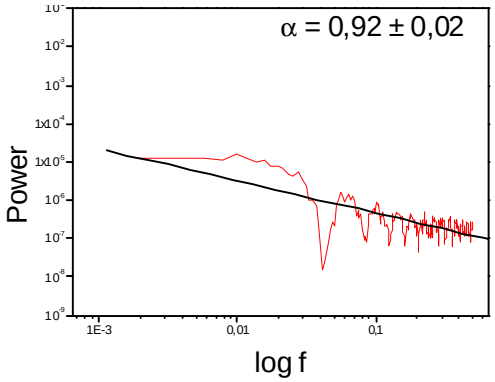

Fig. 6. (a.) Time dependence of stride interval (b.) Power Fourier spectrum of stride intervals

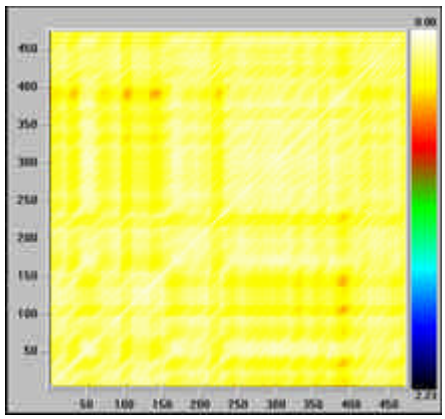

(c.) Recurrence plot of stride intervals

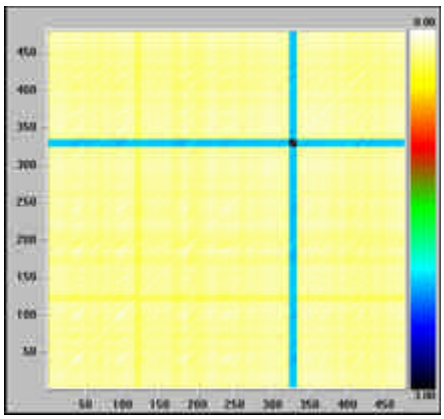

(d.) Randomized recurrence plot

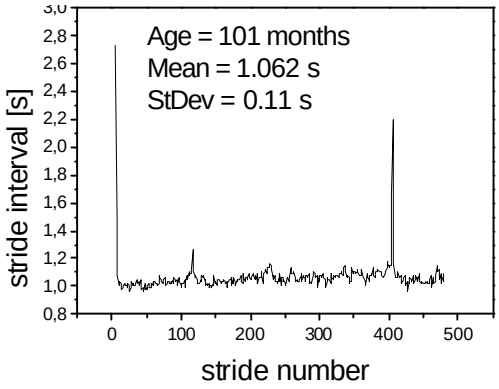

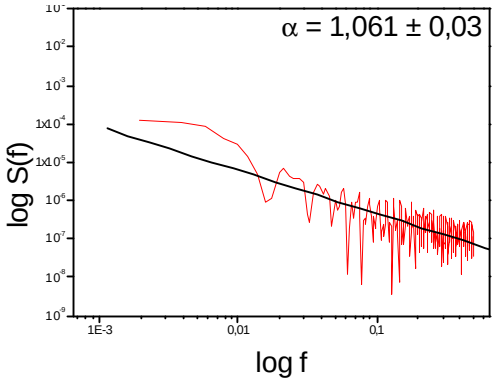

Fig. 7. (a.) Time dependence of stride interval (b.) Power Fourier spectrum of stride intervals

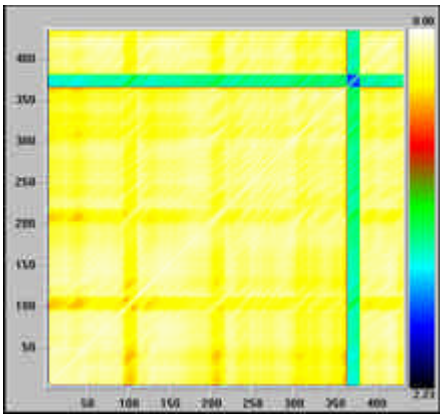

(c.) Recurrence plot of stride intervals

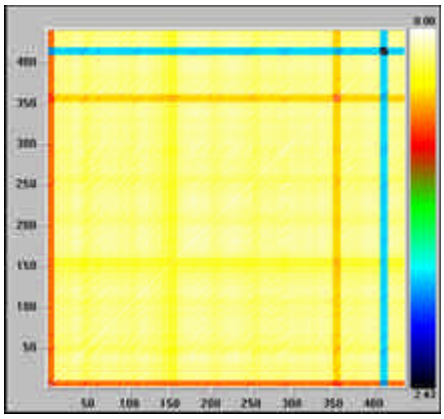

(d.) Randomized recurrence plot

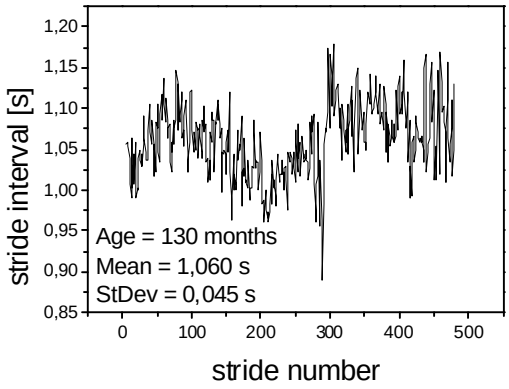

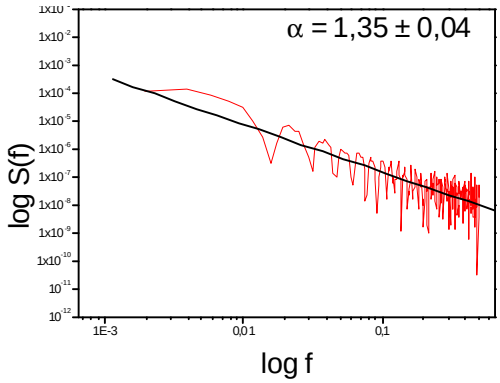

Fig. 8. (a.) Time dependence of stride interval (b.) Power Fourier spectrum of stride intervals

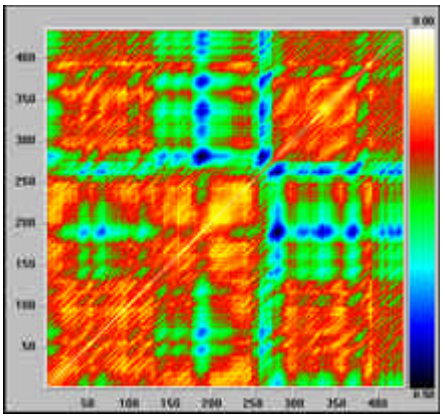

(c.) Recurrence plot of stride intervals

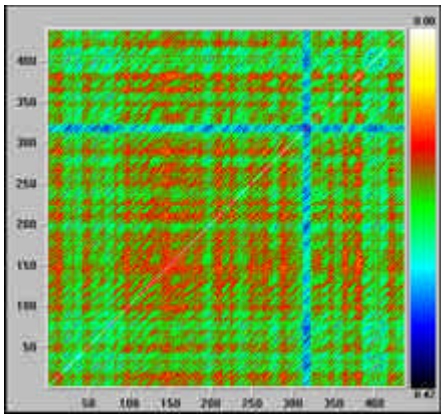

(d.) Randomized recurrence plot

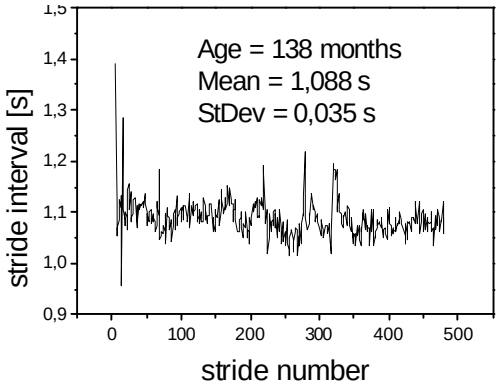

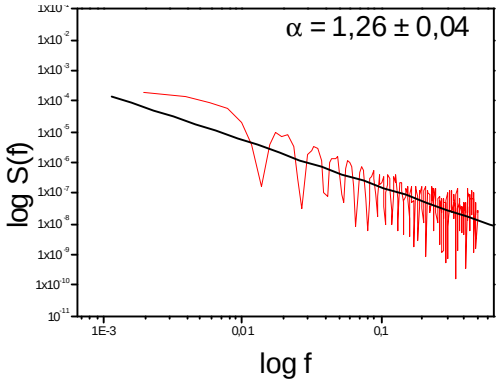

Fig. 9. (a.) Time dependence of stride interval (b.) Power Fourier spectrum of stride intervals

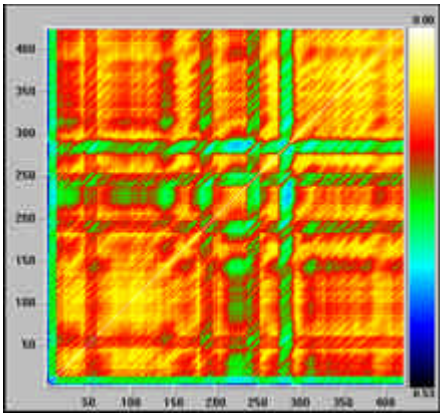

(c.) Recurrence plot of stride intervals

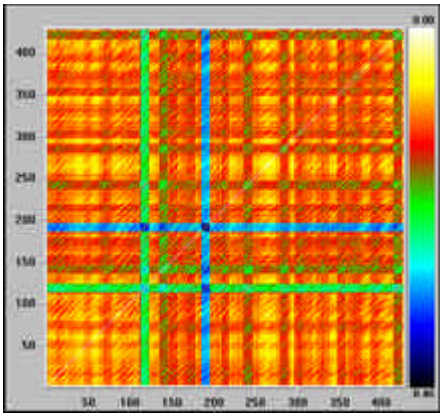

(d.) Randomized recurrence plot

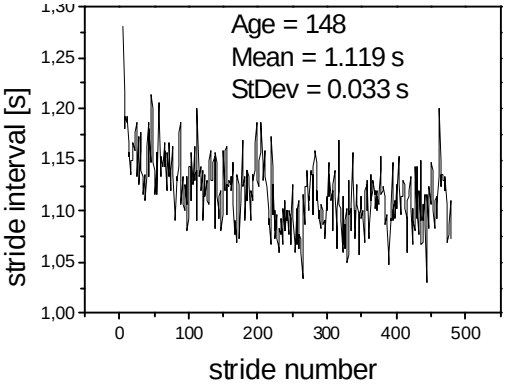

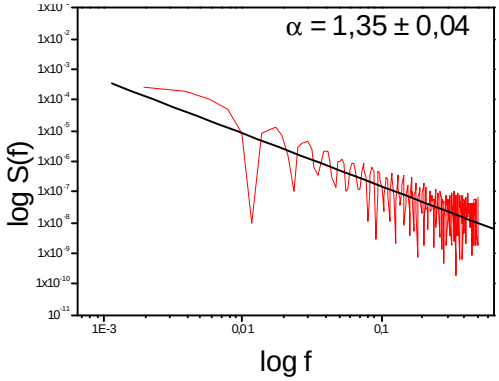

Fig. 10.(a.) Time dependence of stride interval (b.) Power Fourier spectrum of stride intervals

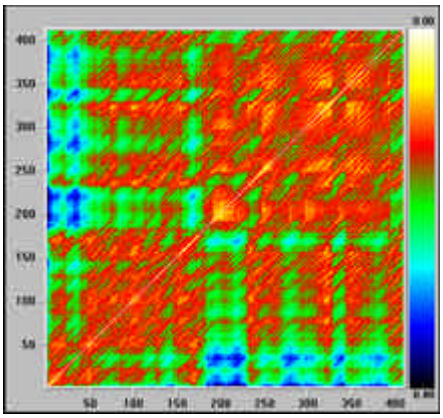

(c.) Recurrence plot of stride intervals

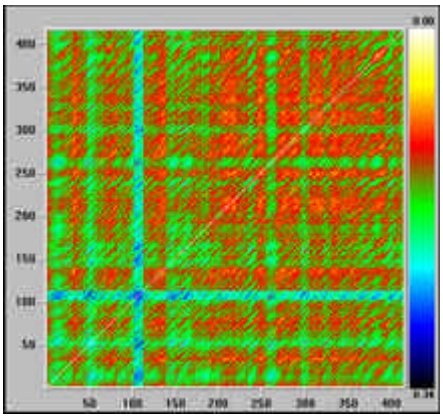

(d.) Randomized recurrence plot

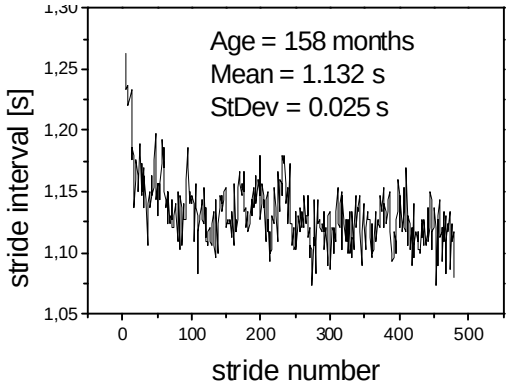

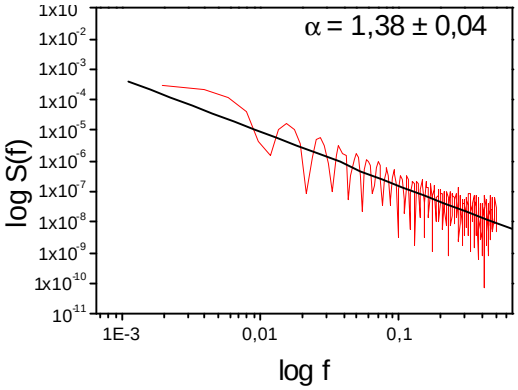

Fig. 11.(a.) Time dependence of stride interval (b.) Power Fourier spectrum of stride intervals

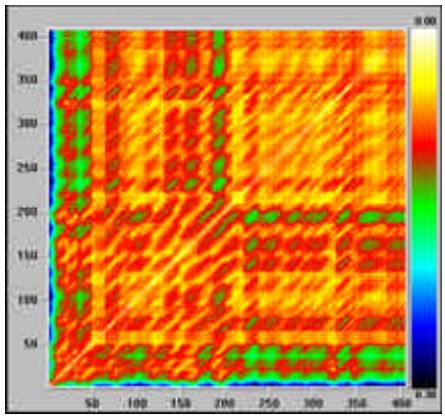

(c.) Recurrence plot of stride intervals

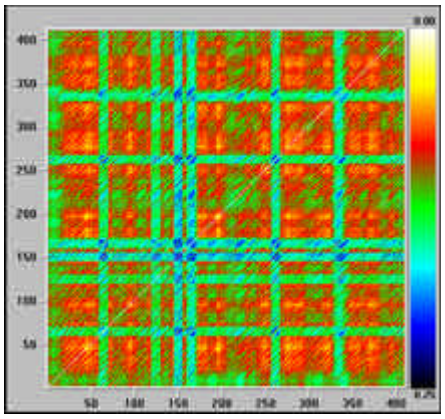

(d.) Randomized recurrence plot

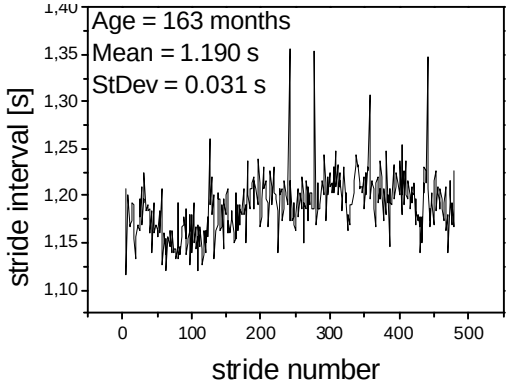

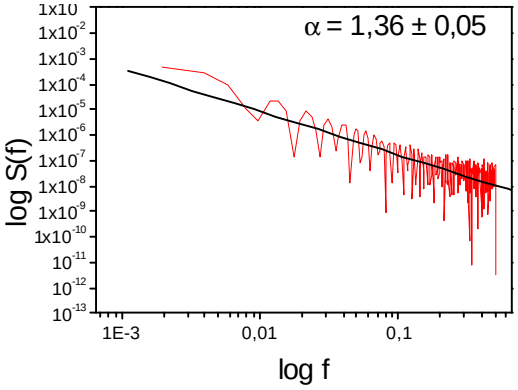

Fig. 12.(a.) Time dependence of stride interval (b.) Power Fourier spectrum of stride intervals

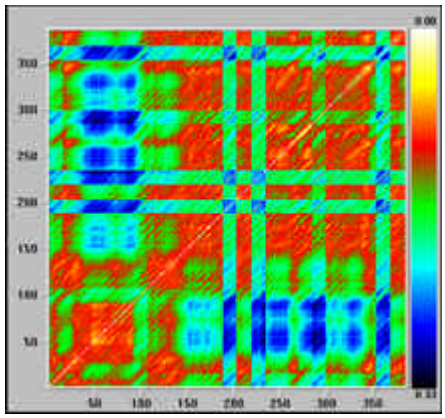

(c.) Recurrence plot of stride intervals

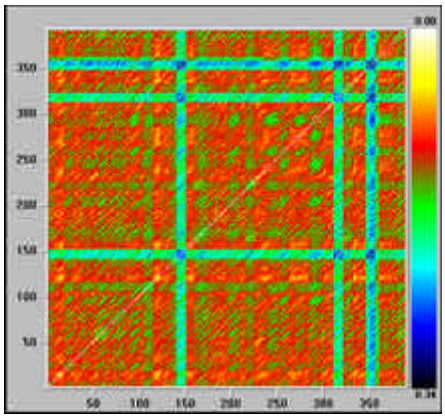

(d.) Randomized recurrence plot

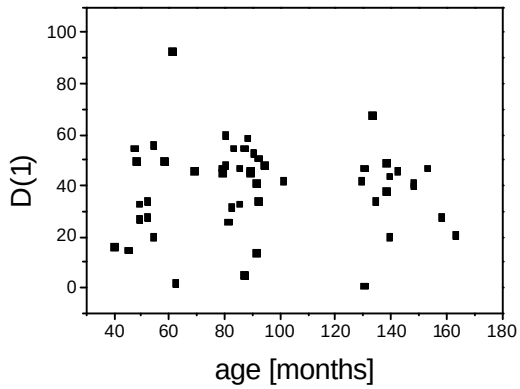

Fig. 13. Age dependence of embedding dimension, time lag = 1

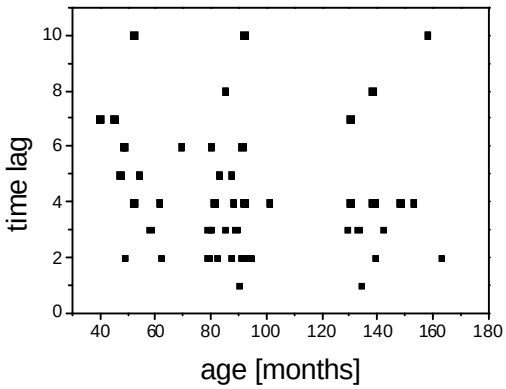

Fig. 14. Age dependence of time lag

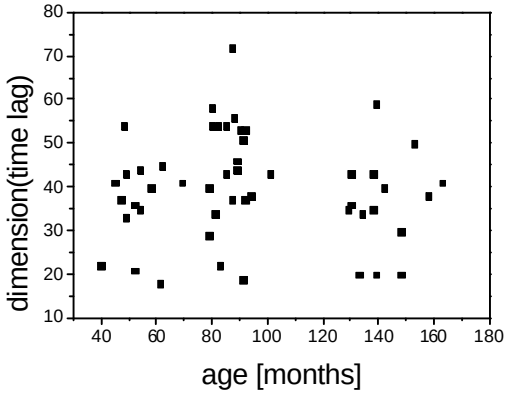

Fig. 15. Age dependence of embedding dimension, time lag is intrinsic value of time series

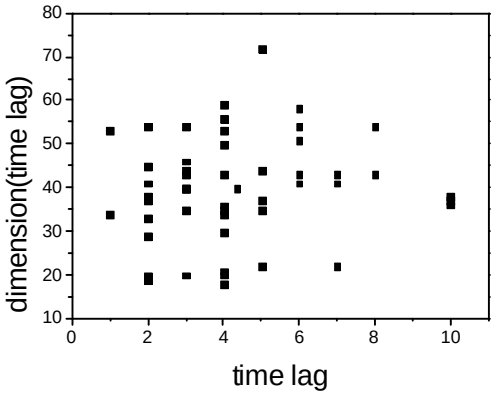

Fig. 16. Dependence of embedding dimension on time lag

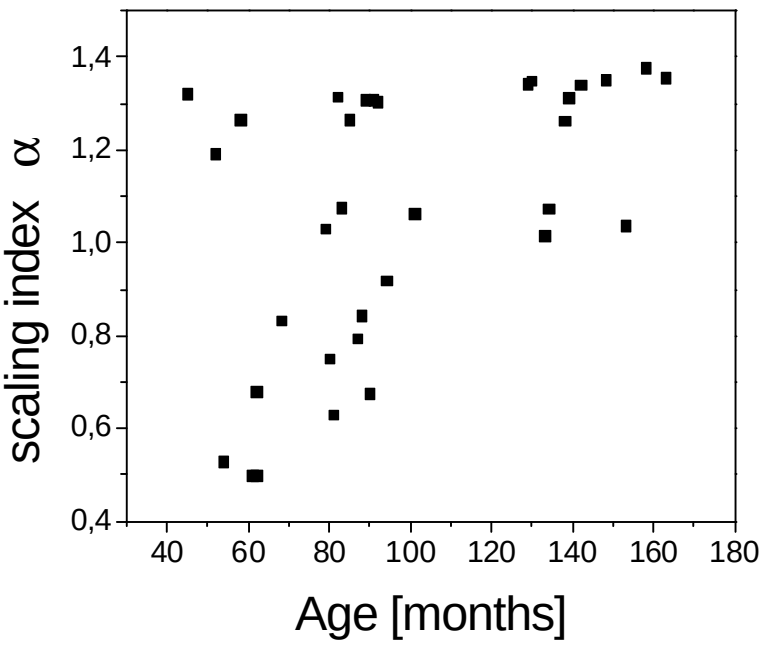

Fig. 17. Age dependence of scaling index a

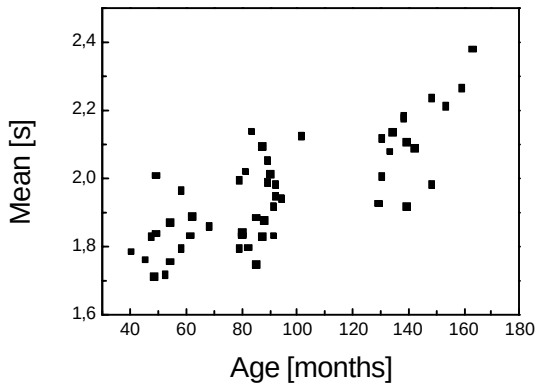

Fig. 18. (a.) Mean of the stride intervals

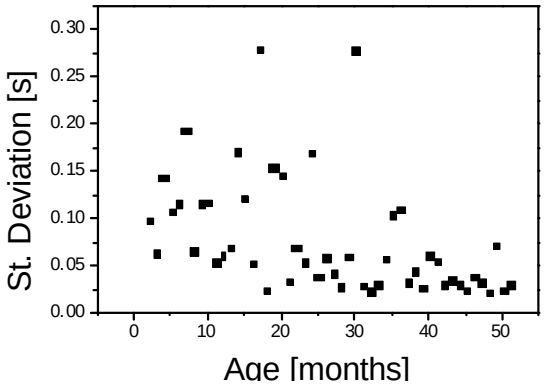

(b.) Age dependence of St. Deviation

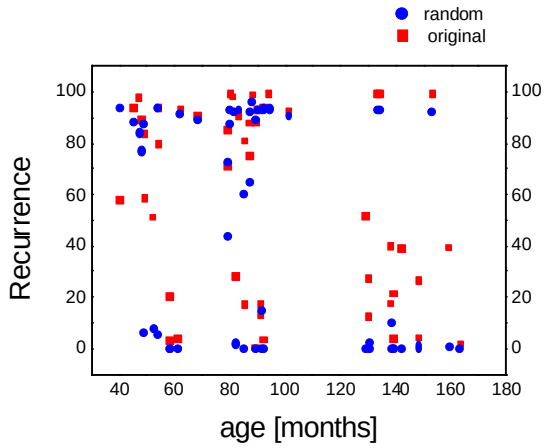

(c.) Age dependence of Recurrence

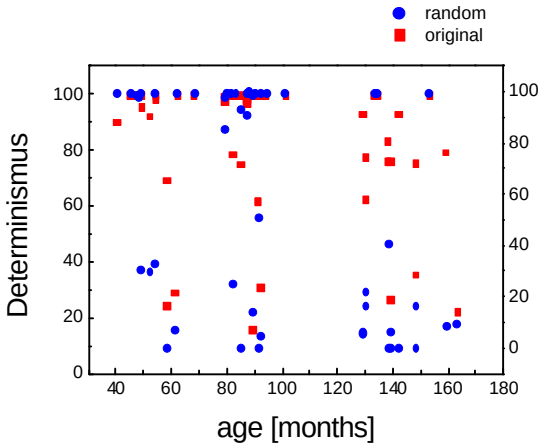

(d.) Age dependence of Determinisms

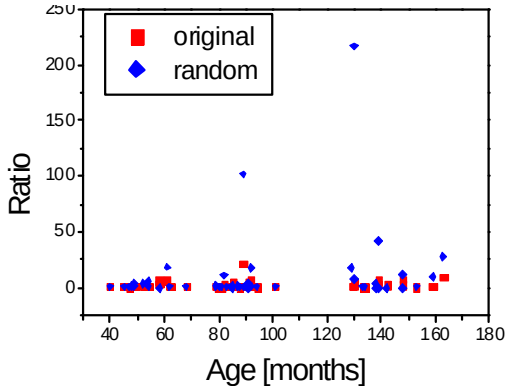

(e.) Age dependence of Ratio

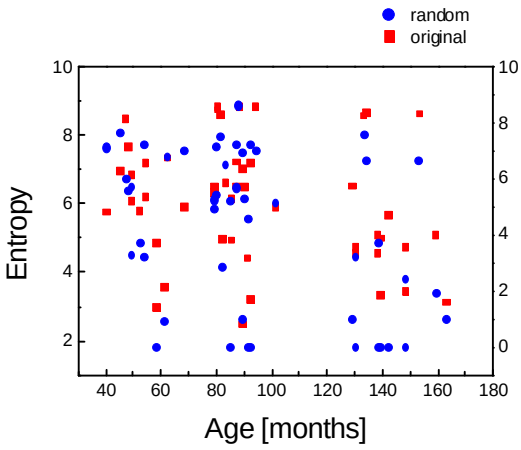

(f.) Age dependence of Entropy

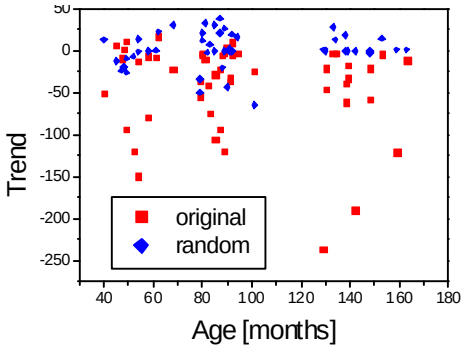

(g.) Age dependence of Trend

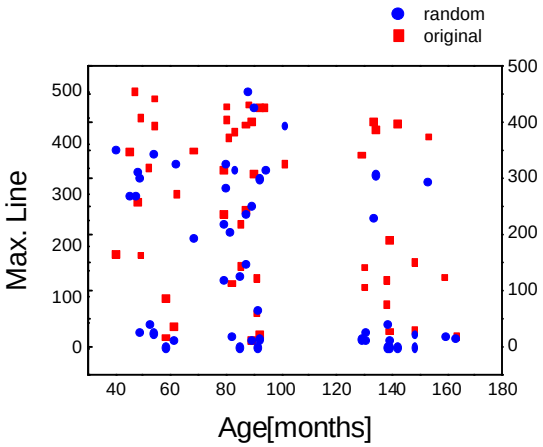

(h.) Age dependence of Max. Line

4.2. Human gait during neurodegenerative diseases (Parkinson, Huntington, and amyotrophic lateral sclerosis)

4.2.1. Analysis of stride intervals and Fourier spectra

Disorders of the basal ganglia are associated with characteristic changes in gait. Patients with Huntington's disease (HD) often display an uncoordinated, lurching walk [Koller, Trimble, 198], while the gait of subjects with Parkinson's disease (PD) is marked by slowness, postural instability, small shuffling steps, and difficulty with initiation [Knutsson, 1972].

On the other hand, amyotrophic lateral sclerosis (ALS) is a disorder primarily affecting the motoneurons of the cerebral cortex, brain stem, and spinal cord. Gait typically becomes abnormal during the course of the disease. A decreased walking velocity has been documented in ALS [Goldfarb, Simon, 1984]. However, it is unknown whether the loss of motoneurons also perturbs the stability and stride intervals.

Our aim in this part of the thesis is to used methods of nonlinear dynamics to enhance the understanding of motor control and might also prove beneficial in monitoring disease progression and in assessing potential therapeutic interventions.

The collection of stride intervals for all diseases was again kindly supplied by Dr. Jeff Haussdorf, Harvard Medical School. Representative examples for ALS, PD, HD, and control healthy subjects (CO), are shown in Figs. 26.-31., Figs. 33.-38, Figs. 40.-45, and Figs. 19.-24, respectively.

For ALS data two features of gait rhythm and stride intervals are visually apparent. First, the average stride time, the time cycle duration, is much longer for the subject with ALS compared with CO subjects. Second, the stride time varies from one stride to the next to a much larger extent in the ALS subject.

For PD subjects the stride-to-stride fluctuations about the mean are larger than that of CO subjects, and these fluctuations are larger in HD subjects. In contrast, the mean values of each time series are similar. Subjects with HD and PD tended to have longer gait cycles and spend more time the feet in contact with the ground.

One possible explanation for increased gait variability, at least in the PD subjects, is that it is a byproduct of lower gait speed. Indeed, many of the gait changes associated with PD are related to diminished ability to generate normal gait stride length

and velocity. However no significant increase in stride intervals was observed in healthy elderly subjects although they walked significantly slower than young controls.

As can be seen from the Figs. 26.b.-31b, 33b-38b, 40b-45b,19b-24b, we have also performed spectral analysis of stride time intervals, and shown power spectra in the log-log scale, in order to determine the fractal scaling exponent α.

4.2.2. Reconstruction of dynamical system behind the stride dynamics

Similarly like for gait maturation we have calculated time lags using AMI method and embedding dimension using FNN method for all PD, HD, ALS and CO subjects. The pairs (time lag, dimension) are shown in the Fig. 48. Average intrinsic time lag was again about 4, but the embedding dimension was in average significantly lower that for young subjects - about 20. Nevertheless a substantial “collapse of dimension” was again not observed and it is not clear if the noise is not such a significant in this case, and therefore is necessary to perform more detailed study to answer this interesting question. Again large differences in embedding dimensions were observed in the same group and also among different various groups. If we have used time lag = 1, the embedding dimension changed only very slightly.

4.2.3. Recurrence quantification analysis

Together with stride intervals and their power Fourier spectra we have again calculated also recurrence plot for original stride intervals series as well as for randomly shuffled data.

Two-dimensional recurrence plots can display ”low-distance” systemic determinism in higher-dimensional stride interval data. The existence of horizontal strips in a recurrence plot is indicative of deterministic structure, possibly chaos. Randomly generated time series data, or even structured data sets, with the order of pairs shuffled so that they still have an equivalent frequency distribution to the original series, will show no patterned structure when plotted as recurrence plots.

The deterministic content of the data was further analysed using data shuffling (global randomization). The more deterministic is the signal, the more is the plot changed.

As can be seen in some recurrence plots are present short lines parallel to the main diagonal. They corresponds to sequences (i, j), (i+1, j+1), ..., (i+k, j+k) such that the piece of trajectory x(j), x(j+1),...,x(j+k), is close to trajectory x(i), x(i+1), ..., x(i+k). The length of the lines is thus related to the inverse of the largest Lyapunov exponent. The presence of these short segments mirrors the deterministic character of the system and it follows directly from the presence of so-called unstable periodical orbits that are embedded in the chaotic attractor of a system. If the x(i) were randomly chosen rather than coming from a dynamical system, there would be no such lines.

HD patients exhibited more gait variability than PD subjects. This may reflect the impairment of different neural pathways involved in stride-to-stride regulation, consistent with numerous differences in the gait of PD and HD subjects. Alternatively, the origin of the increased variability may be the same in PD and HD and the differences are merely a matter of degree. Although the underlying pathology of each disease involves different portions of the basal ganglia, both diseases share some common sequel that may be the primary reason for the impairment in regulation of gait timing.

It is likely that complex dynamics of the gait stride intervals from numerous coupled control systems and feedback loops that regulate the gait cycle on different time scales. Neurodegenerative diseases may have a profound impact on many of the interacting neural and endocrine mechanisms that regulate gate.

These results suggests that the distinctive patterns evident in RPs of stride intervals, are empirically correlated with the age and health of the studied subjects, as they diagrammatically represent the complex dynamical interaction of the neuro-muscular systems. These findings suggest that recurrence plots of stride interval variability, show patterns which vary characteristically, for different types of people, in the different states, able to differentiate healthy or ill, old and young subjects.

Our further goal is to evaluate if recurrence plots of stride intervals of subjects with various disorders actually have potential as a clinical diagnostic tool.

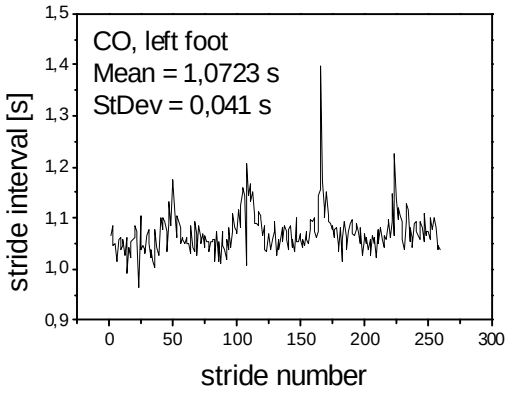

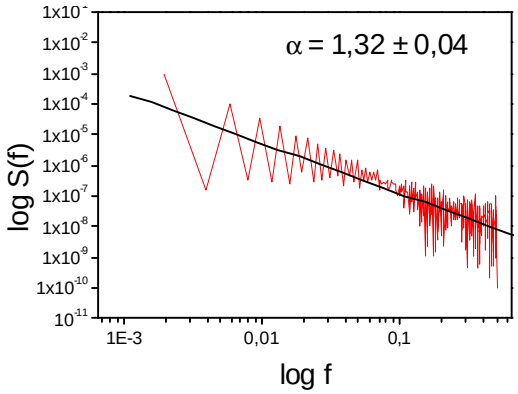

Fig.19.(a.) Time dependence of stride interval (b.) Power Fourier spectrum of stride intervals

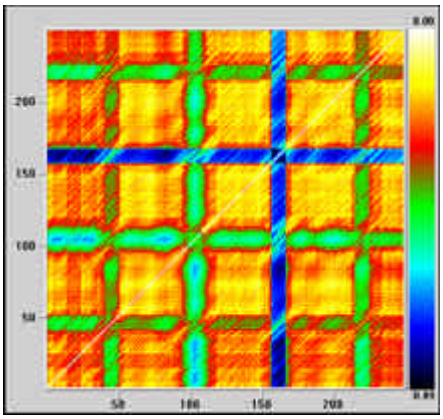

(c.) Recurrence plot of stride intervals

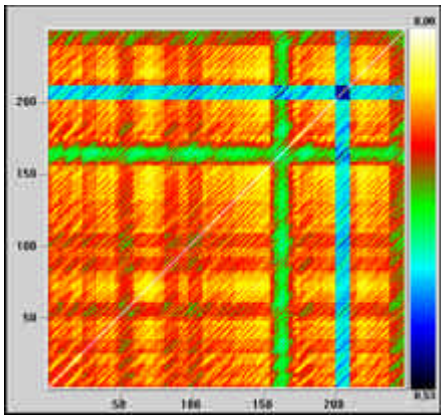

(d.) Randomized recurrence plot

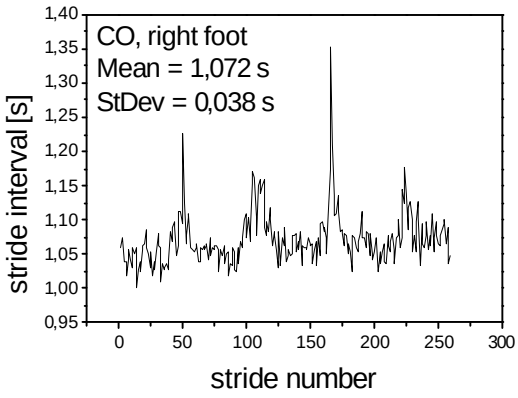

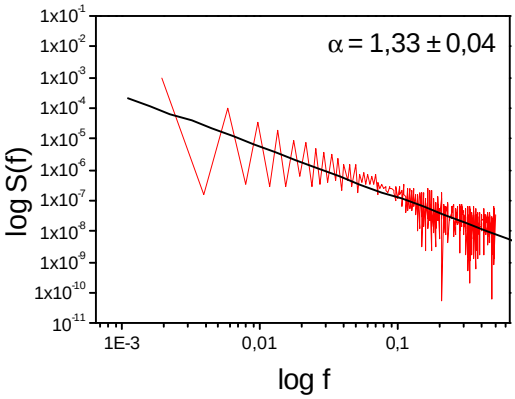

Fig.20 (a.) Time dependence of stride interval (b.) Power Fourier spectrum of stride intervals

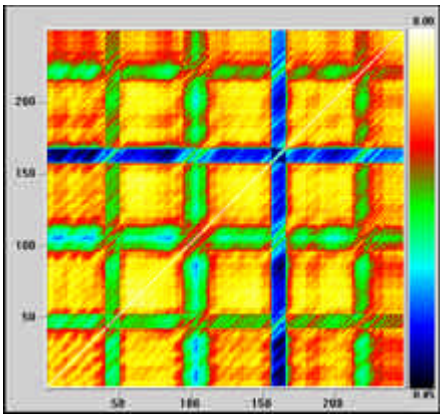

(c.) Recurrence plot of stride intervals

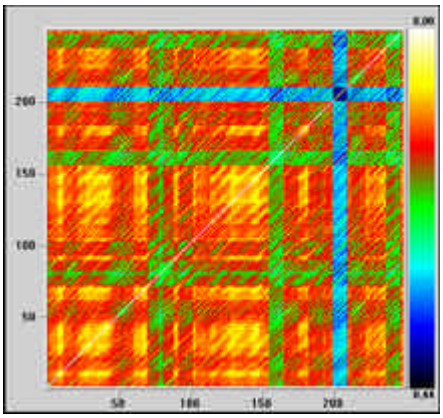

(d.) Randomized recurrence plot

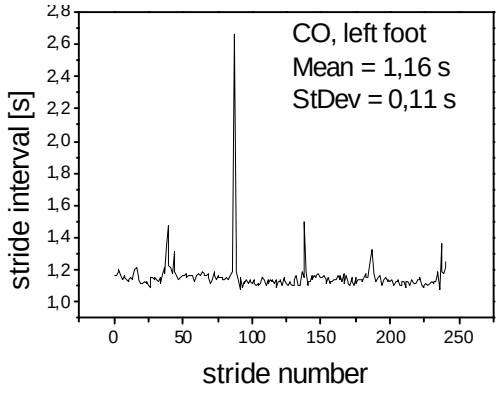

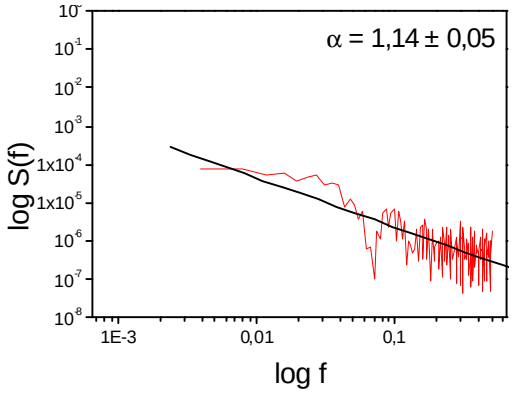

Fig.21.(a.) Time dependence of stride interval (b.) Power Fourier spectrum of stride intervals

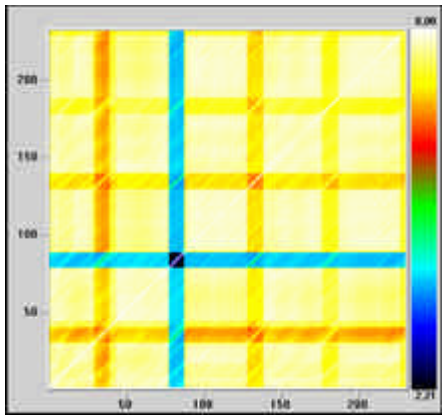

(c.) Recurrence plot of stride intervals

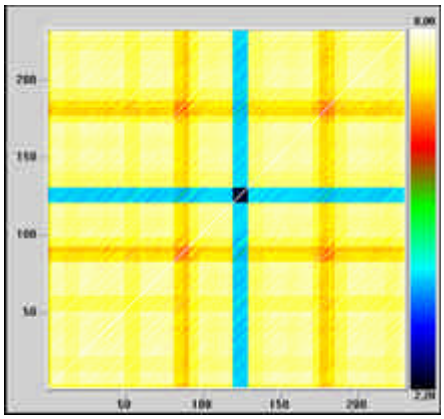

(d.) Randomized recurrence plot

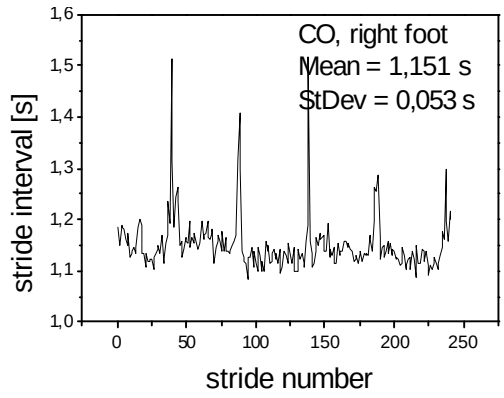

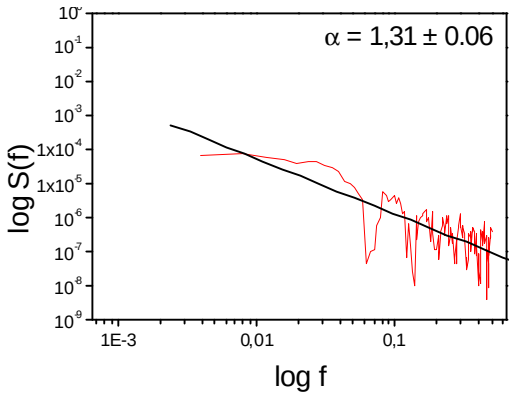

Fig.22. (a.) Time dependence of stride interval (b.) Power Fourier spectrum of stride intervals

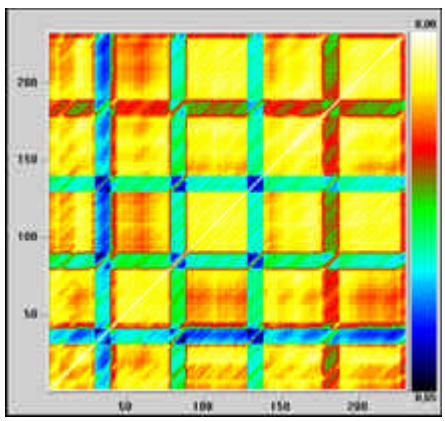

(c.) Recurrence plot of stride intervals

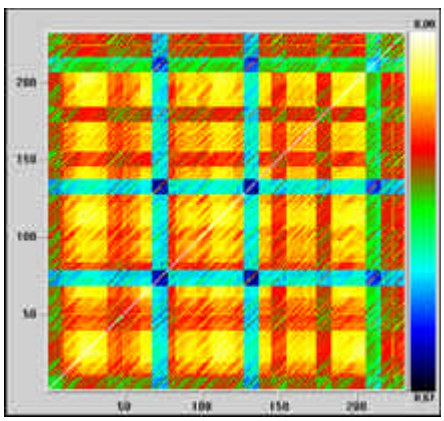

(d.) Randomized recurrence plot

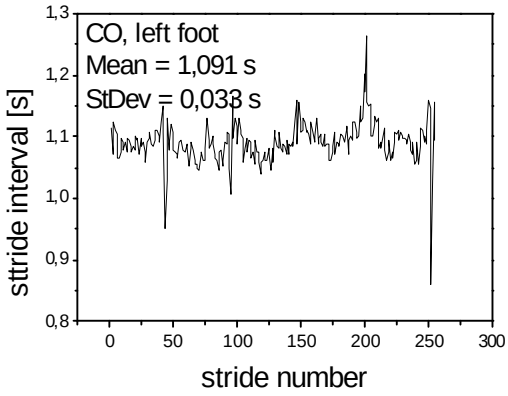

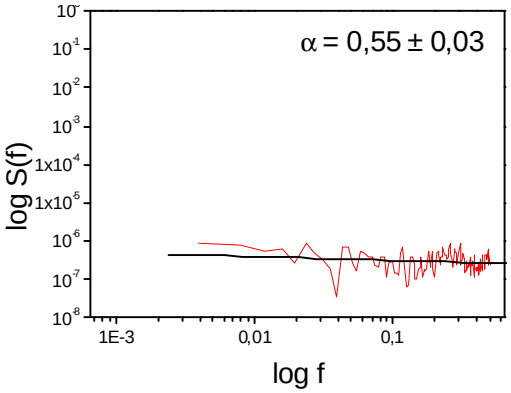

Fig.23. (a.) Time dependence of stride interval (b.) Power Fourier spectrum of stride intervals

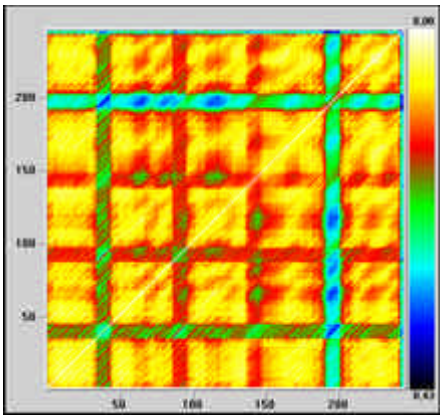

(c.) Recurrence plot of stride intervals

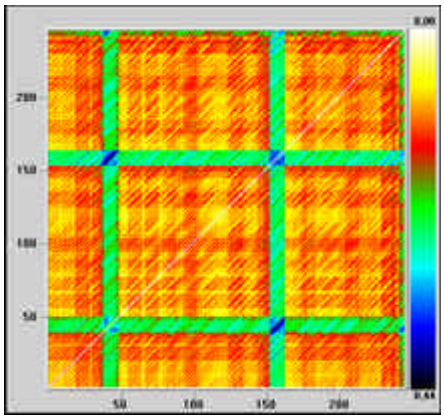

(d.) Randomized recurrence plot

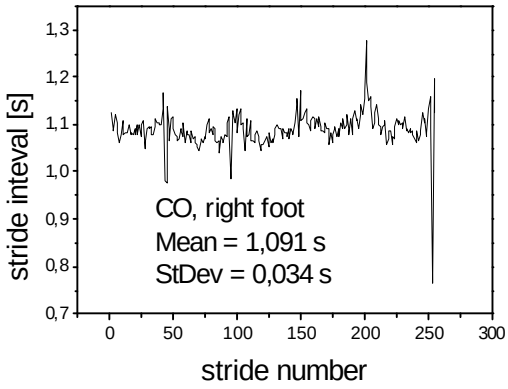

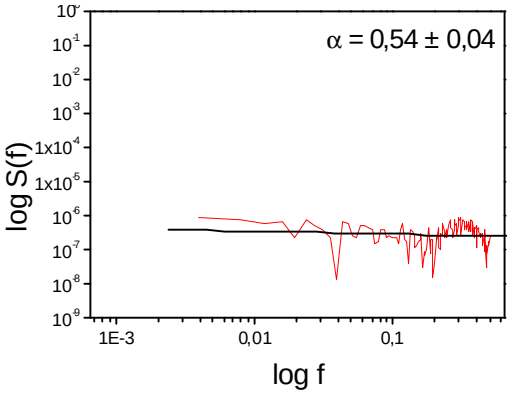

Fig.24. (a.) Time dependence of stride interval (b.) Power Fourier spectrum of stride intervals

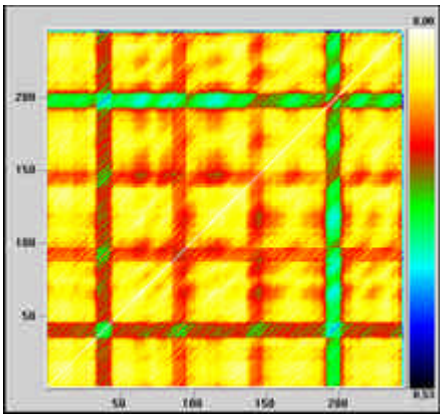

(c.) Recurrence plot of stride intervals

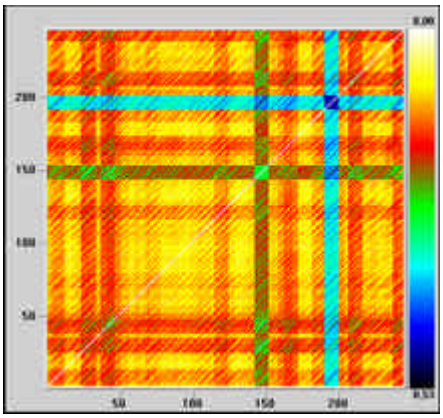

(d.) Randomized recurrence plot

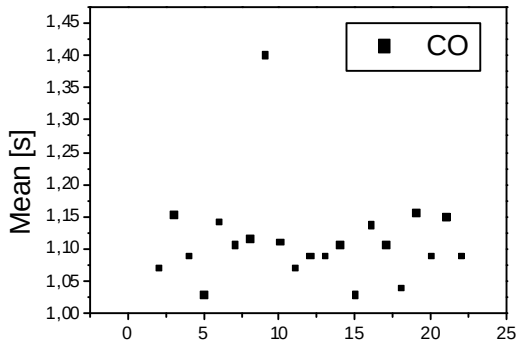

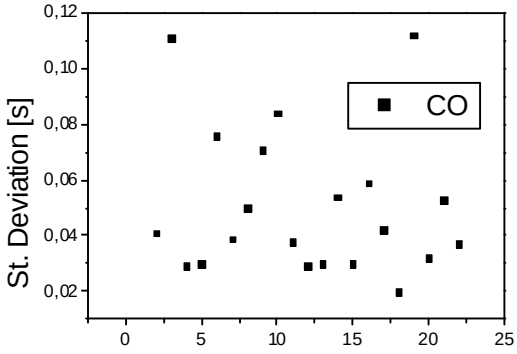

Fig. 25. (a.) Mean of the stride intervals (b.) Standard deviation of stride intervals

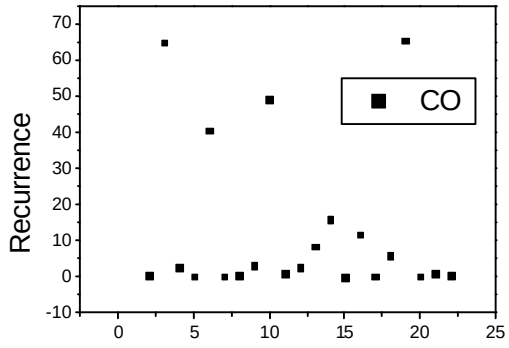

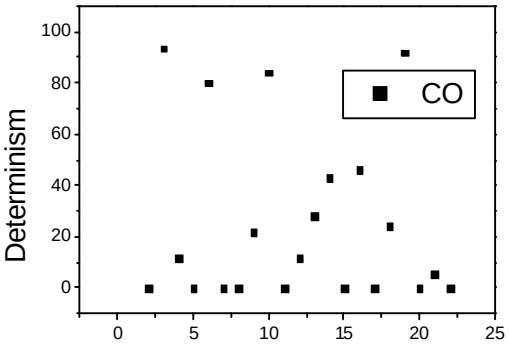

(c) Recurrence of healthy people (d.) Determinism of heathly people

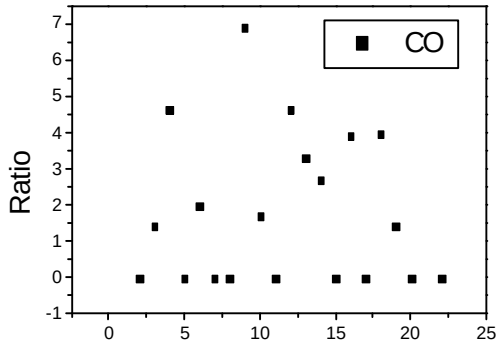

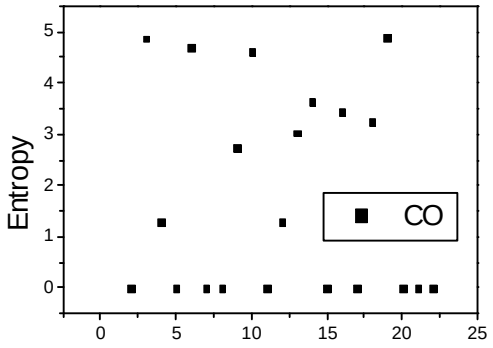

(e.) Ratio of healthy people (f.) Entropy of healthy people

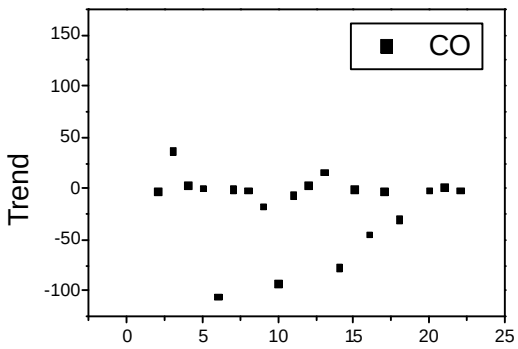

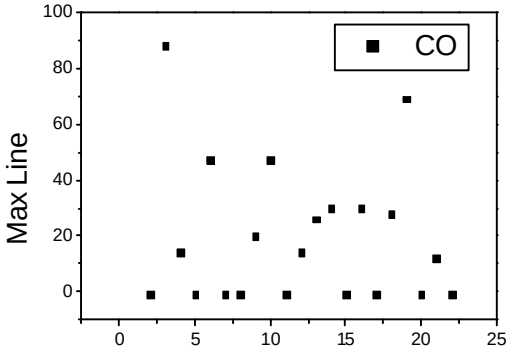

(g.) Trend of healthy people (h.) Max. Line of healthy people

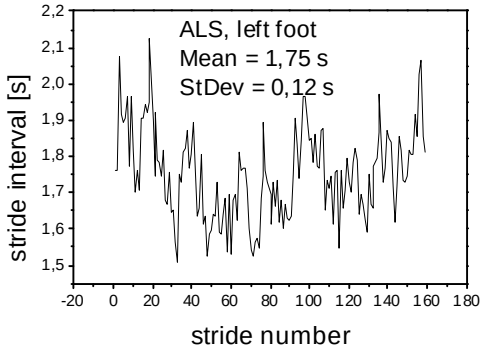

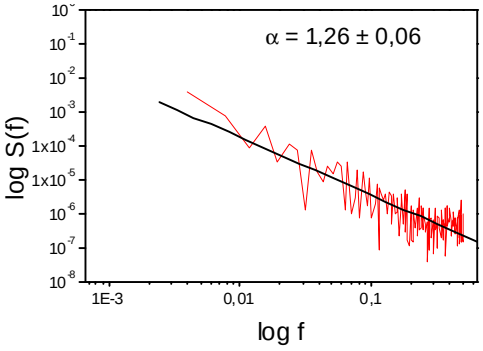

Fig.26. (a.) Time dependence of stride interval (b.) Power fourier spectrum of stride intervals

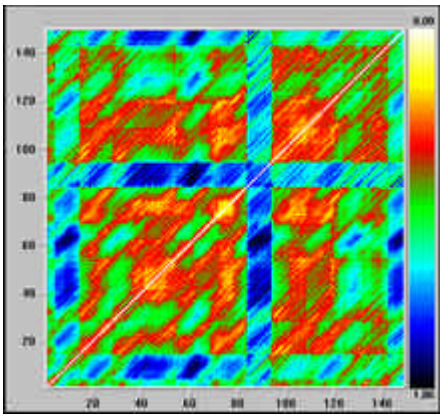

(c.) Recurrence plot of stride intervals

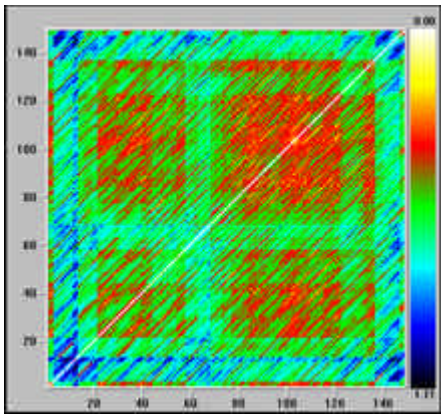

(d.) Randomized recurrence plot

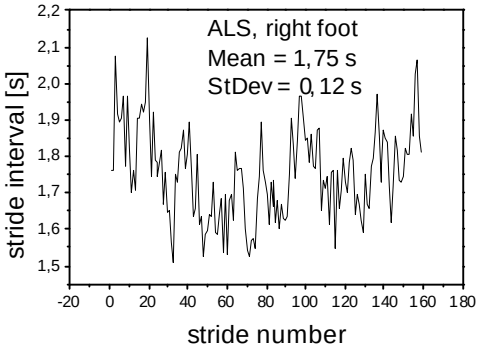

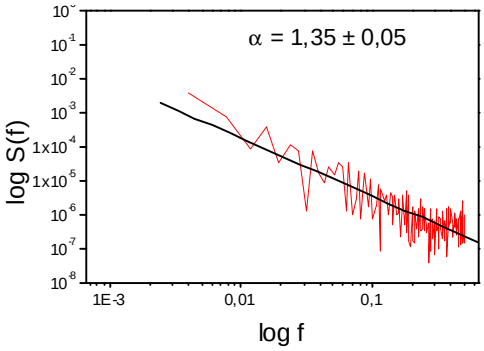

Fig27. (a.) Time dependence of stride interval (b.) Power fourier spectrum of stride intervals

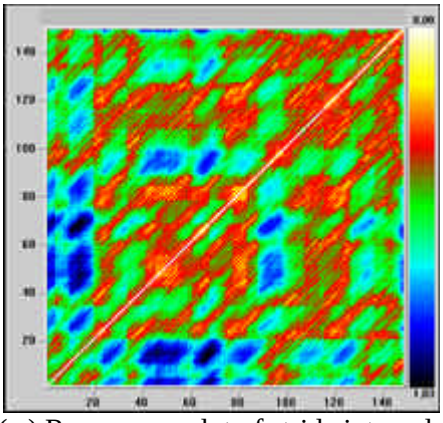

(c.) Recurrence plot of stride intervals

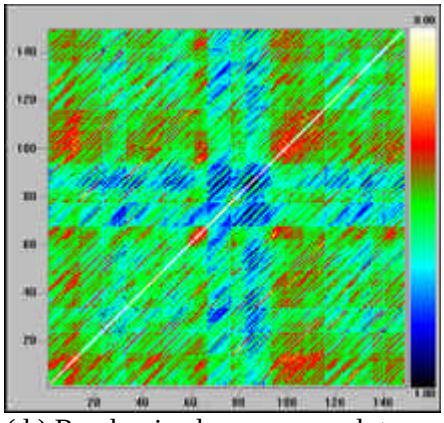

(d.) Randomized recurrence plot

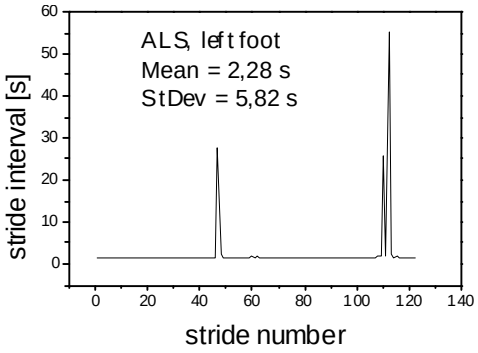

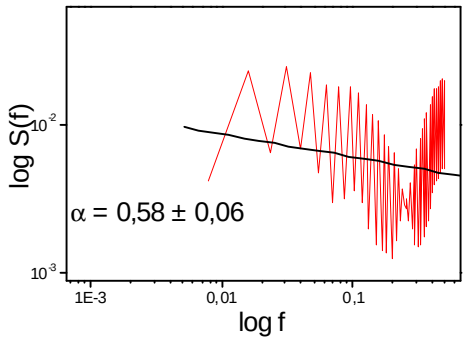

Fig.28. (a.) Time dependence of stride interval (b.) Power fourier spectrum of stride intervals

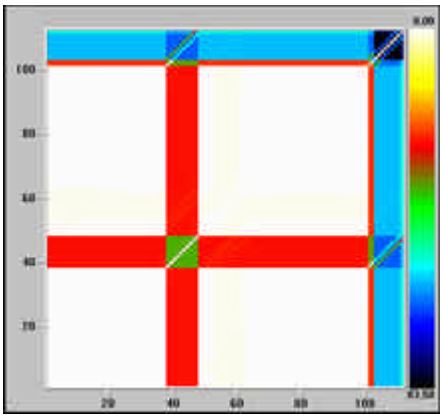

(c.) Recurrence plot of stride intervals

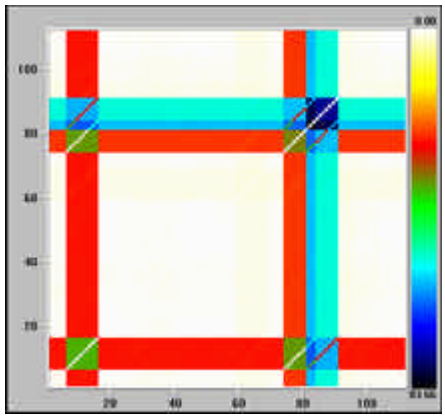

(d.) Randomized recurrence plot

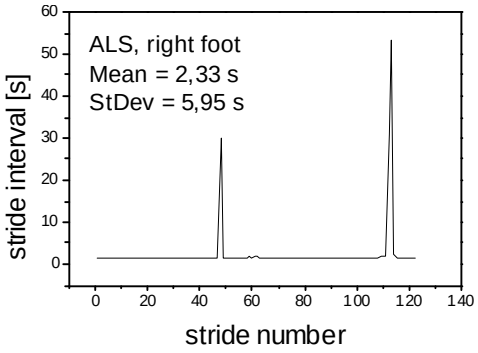

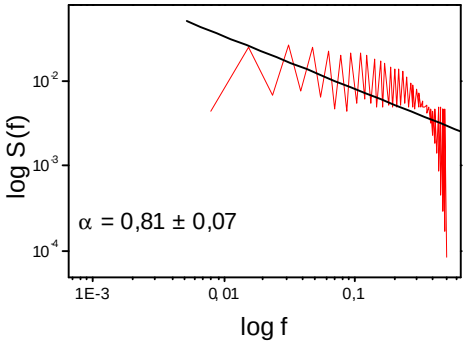

Fig.29. (a.) Time dependence of stride interval (b.) Power fourier spectrum of stride intervals

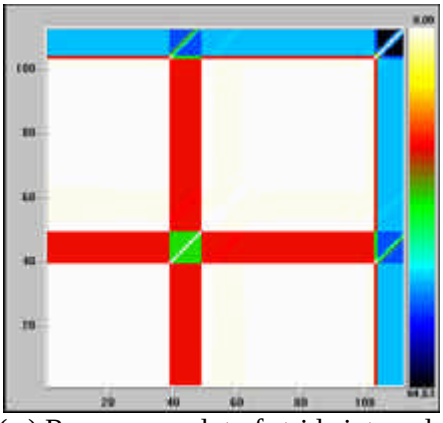

(c.) Recurrence plot of stride intervals

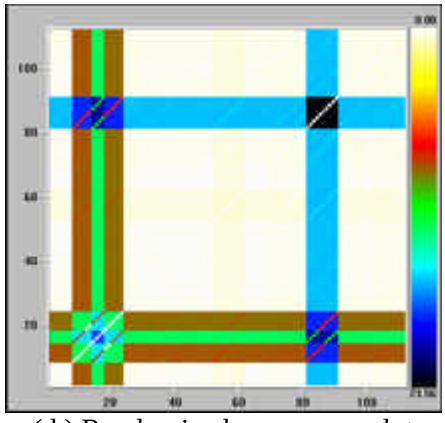

(d.) Randomized recurrence plot

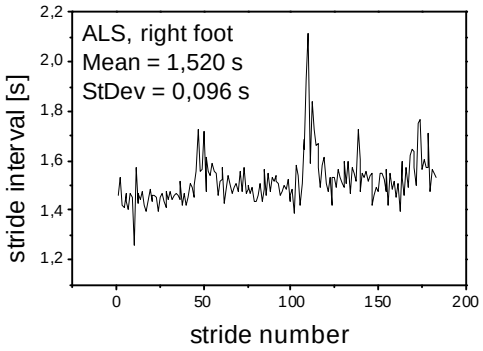

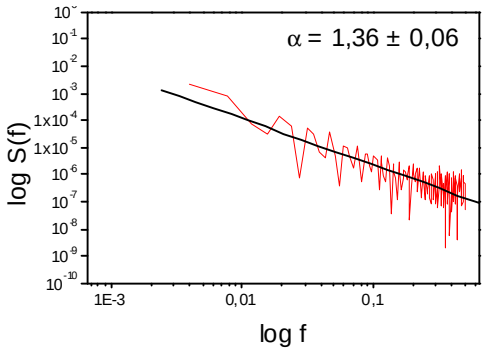

Fig. 30 (a.) Time dependence of stride interval (b.) Power fourier spectrum of stride intervals

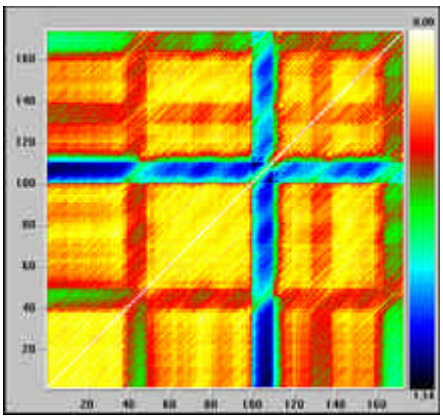

(c.) Recurrence plot of stride intervals

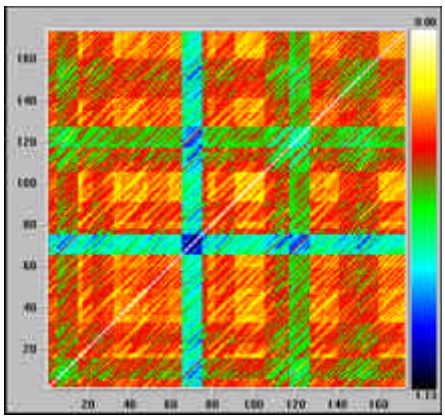

(d.) Randomized recurrence plot

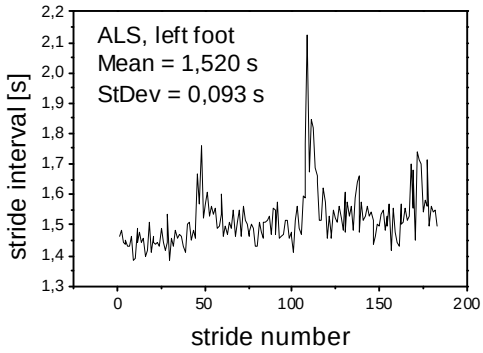

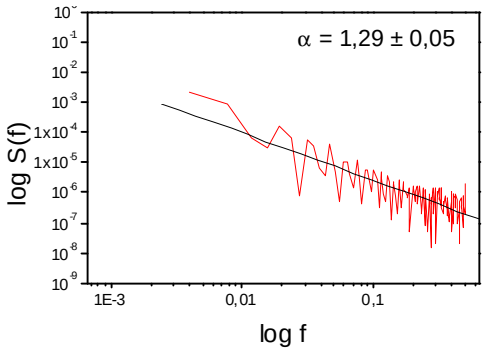

Fig. 31 (a.) Time dependence of stride interval (b.) Power fourier spectrum of stride intervals

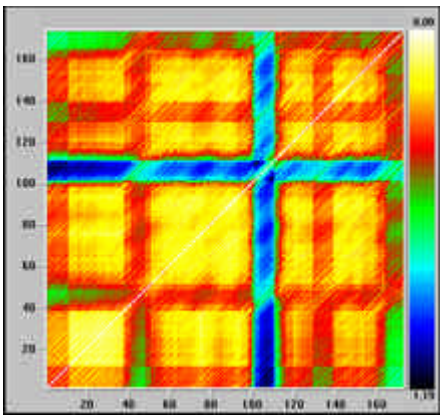

(c.) Recurrence plot of stride intervals

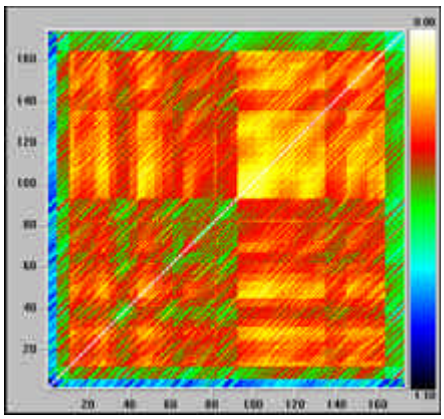

(d.) Randomized recurrence plot

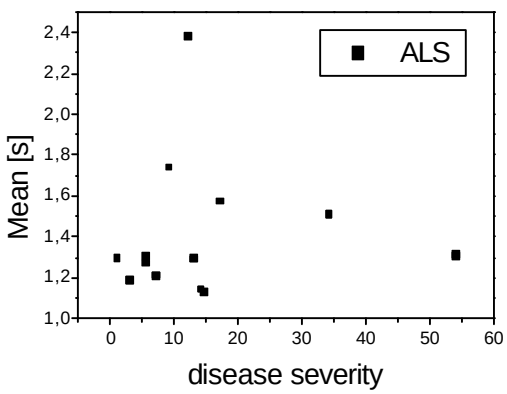

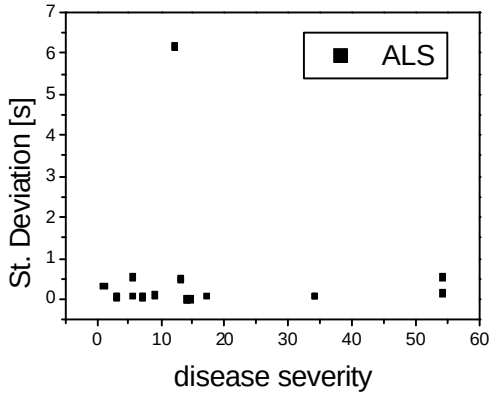

Fig.32. (a.) Mean of the stride intervals (b.) St. Deviation of stride intervals of ALS

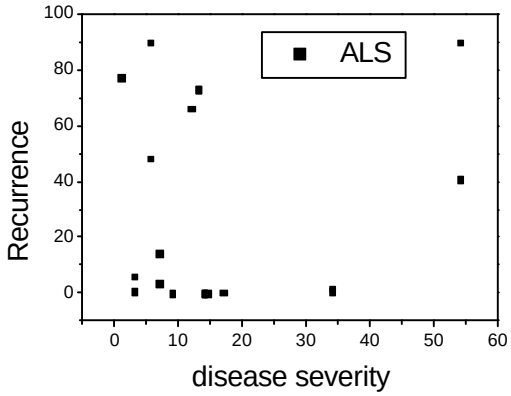

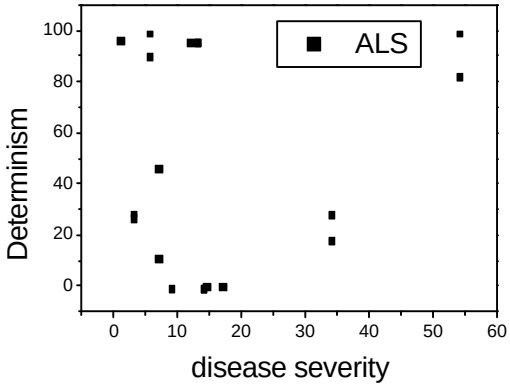

(c.) Recurrence of ALS (d.) Determinism of ALS

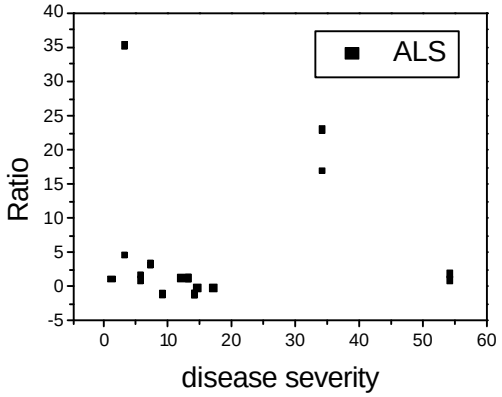

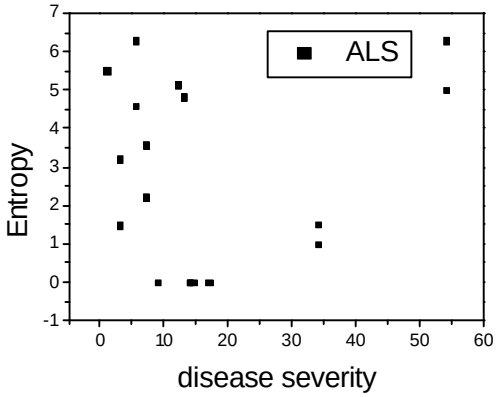

(e.) Ratio of ALS (f.) Entropy of ALS

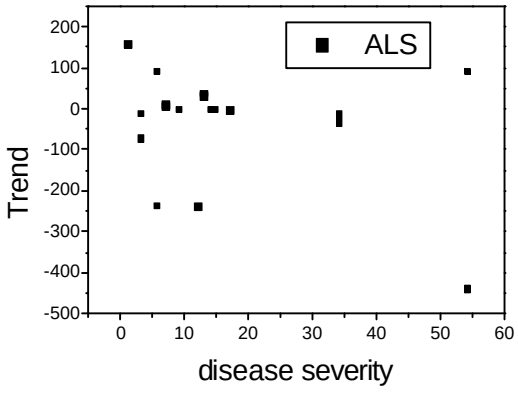

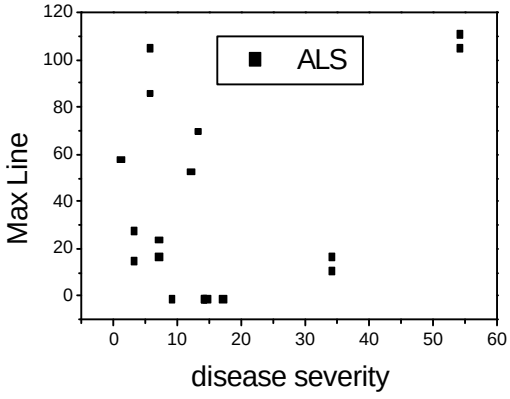

(g.) Trend of ALS (h.) Max. Line of ALS

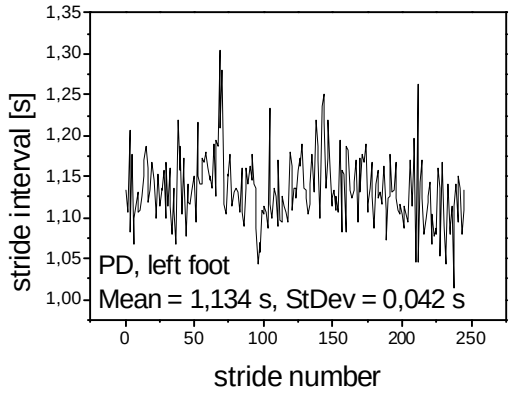

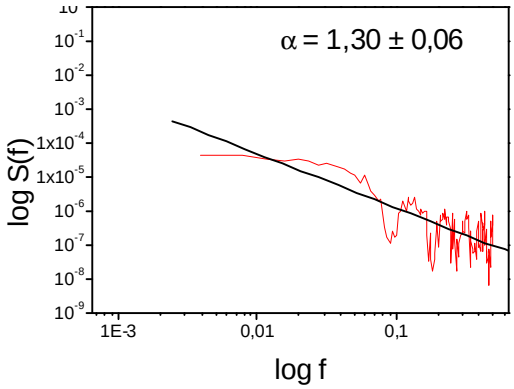

Fig.33. (a.) Time dependence of stride interval (b.) Power fourier spectrum of stride intervals

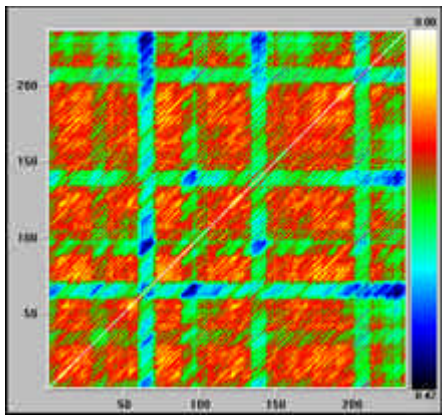

(c.) Recurrence plot of stride intervals

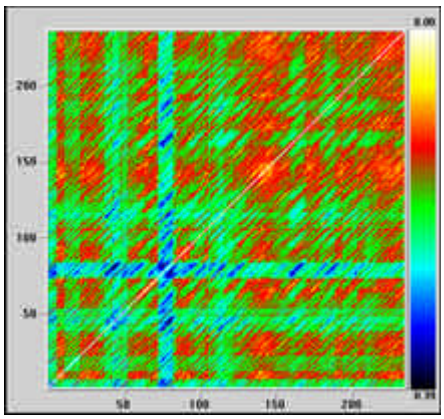

(d.) Randomized recurrence plot

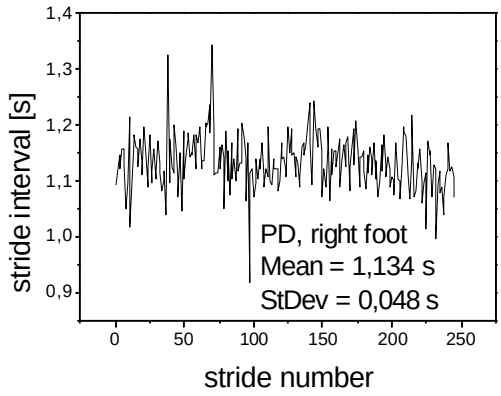

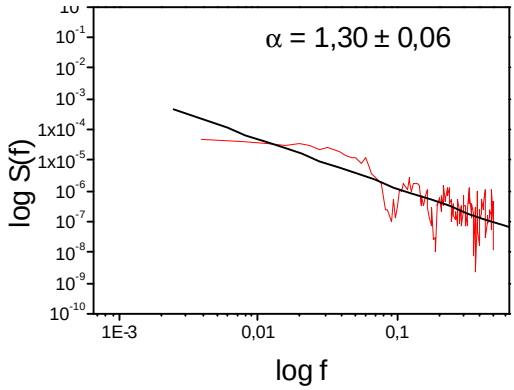

Fig.34. (a.) Time dependence of stride interval (b.) Power fourier spectrum of stride intervals

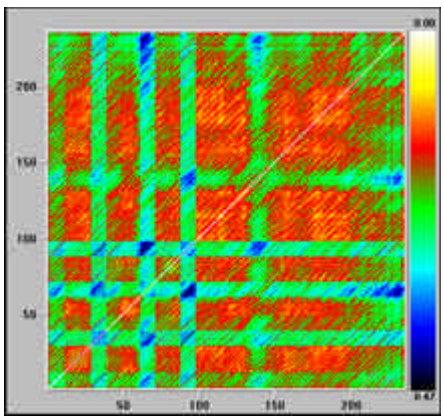

(c.) Recurrence plot of stride intervals

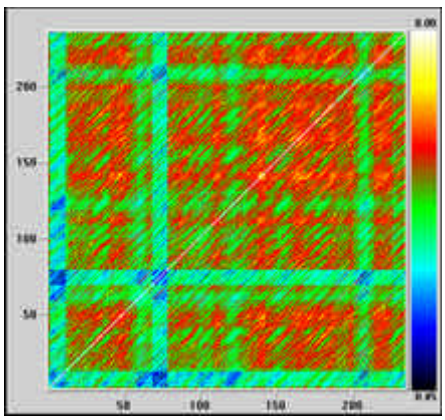

(d.) Randomized recurrence plot

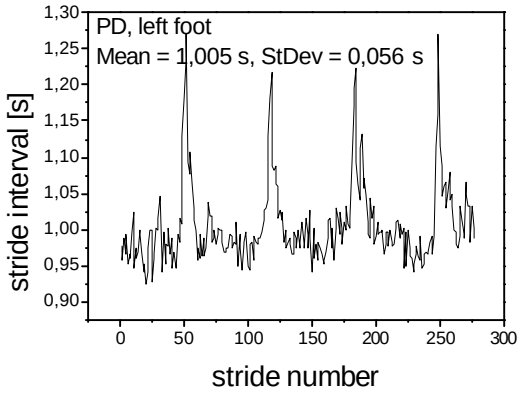

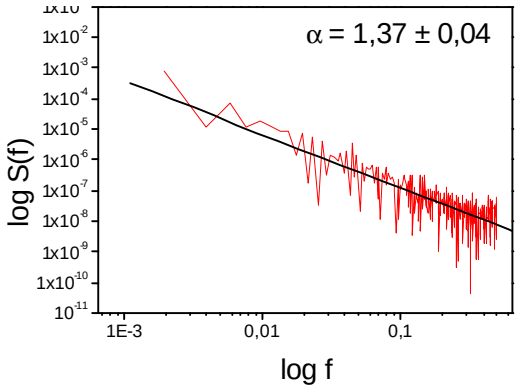

Fig.35. (a.) Time dependence of stride interval (b.) Power fourier spectrum of stride intervals

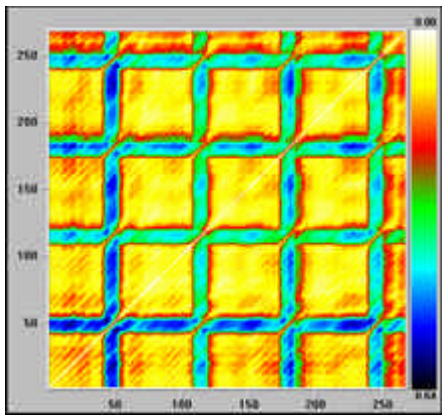

(c.) Recurrence plot of stride intervals

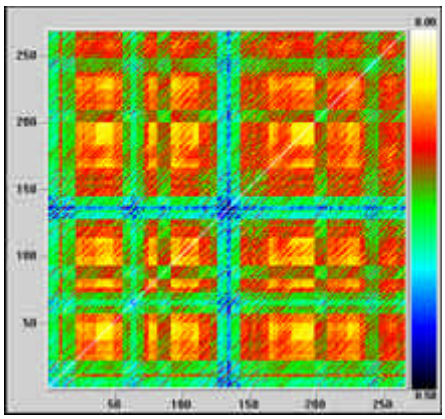

(d.) Randomized recurrence plot

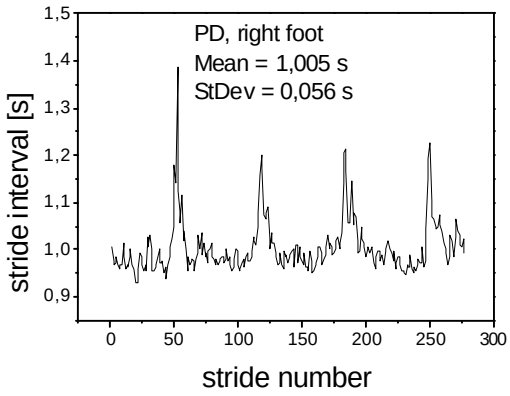

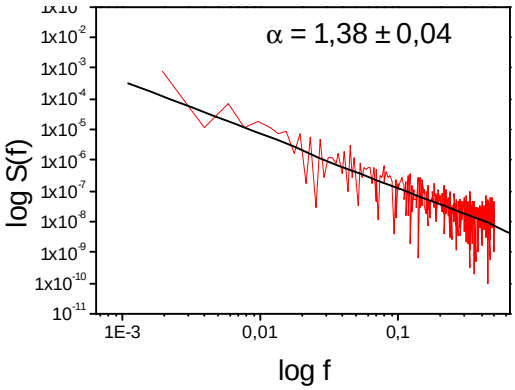

Fig.36. (a.) Time dependence of stride interval (b.) Power fourier spectrum of stride intervals

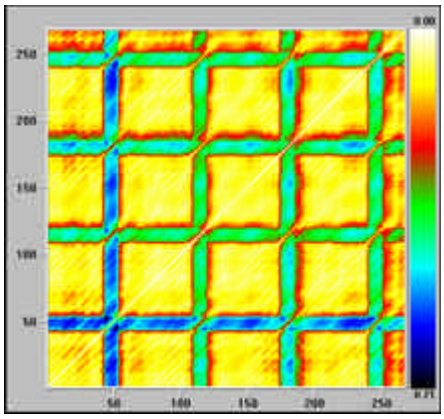

(c.) Recurrence plot of stride intervals

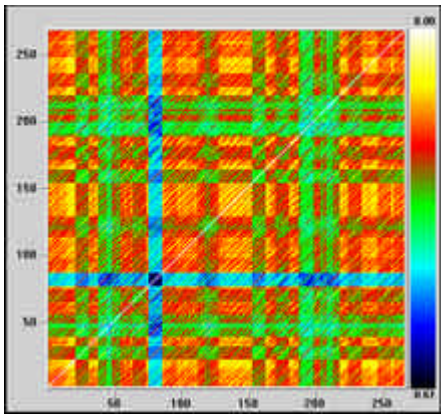

(d.) Randomized recurrence plot

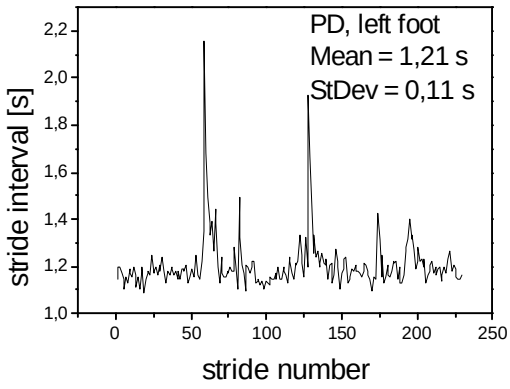

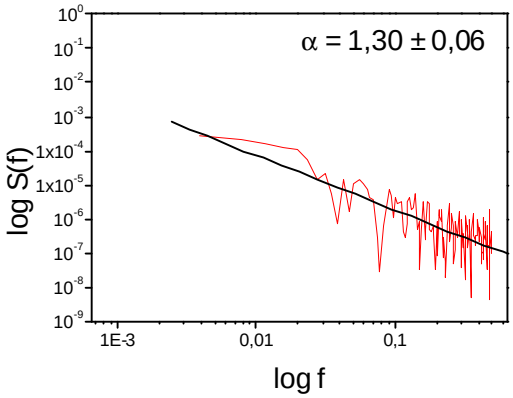

Fig.37. (a.) Time dependence of stride interval (b.) Power fourier spectrum of stride intervals

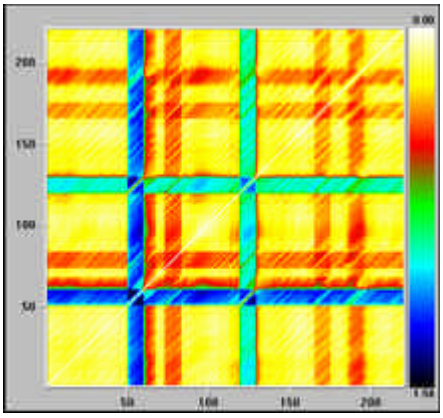

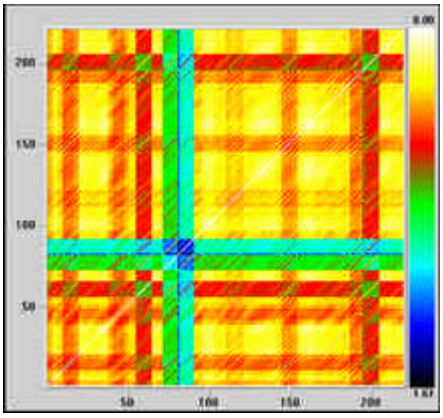

(c.) Recurrence plot of stride intervals (d.) Randomized recurrence plot

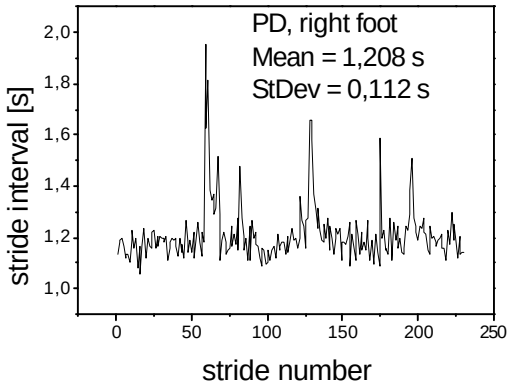

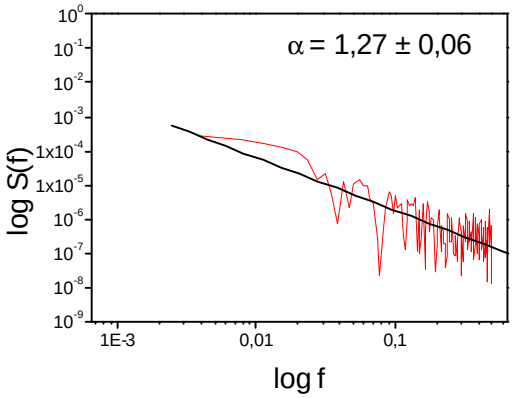

Fig.38. (a.) Time dependence of stride interval (b.) Power fourier spectrum of stride intervals

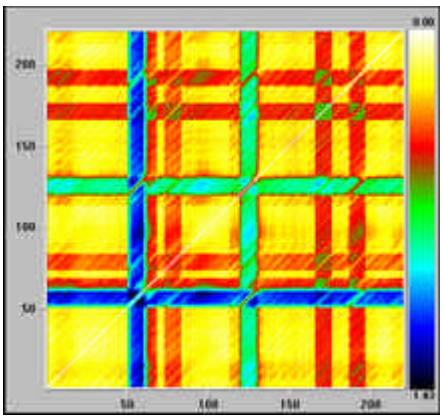

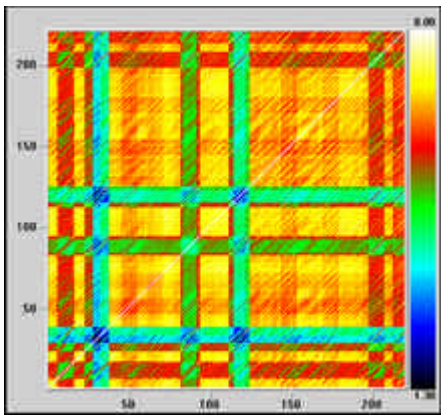

(c.) Recurrence plot of stride intervals (d.) Randomized recurrence plot

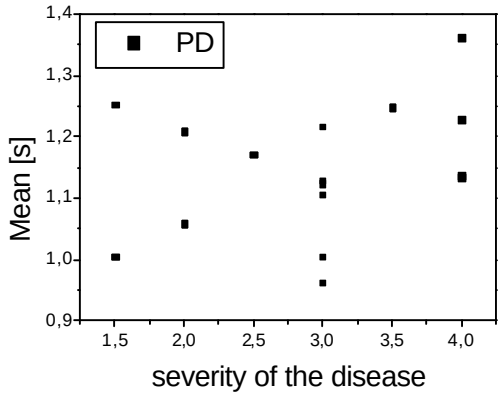

Fig.39. (a.) Mean of the stride intervals

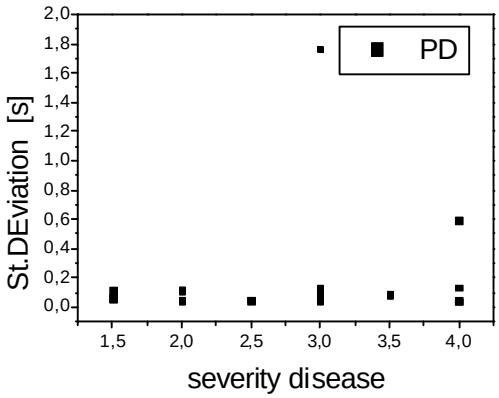

(b.) St. Deviation of stride intervals

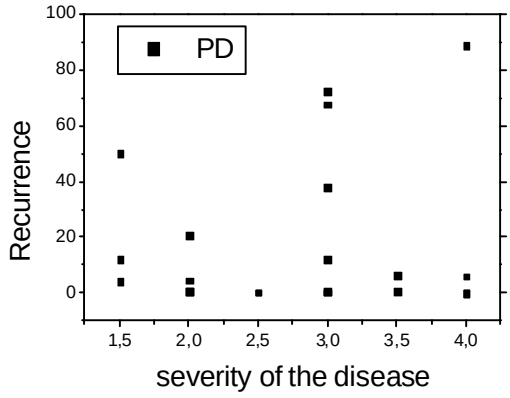

(c.) Recurrence of PD

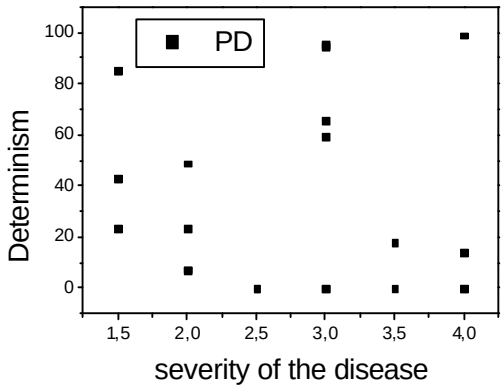

(d.) Determinism of PD

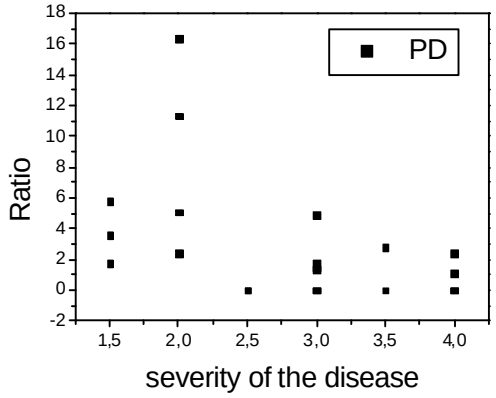

(e.) Ratio of PD

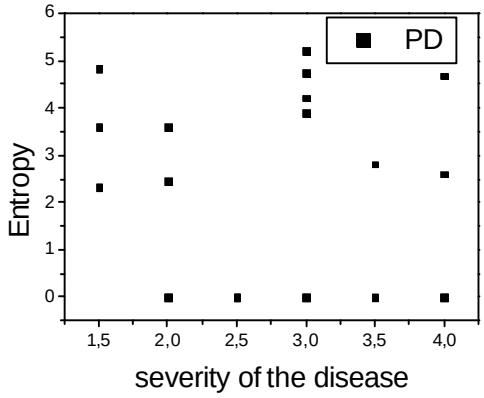

(f.) Entropy of PD

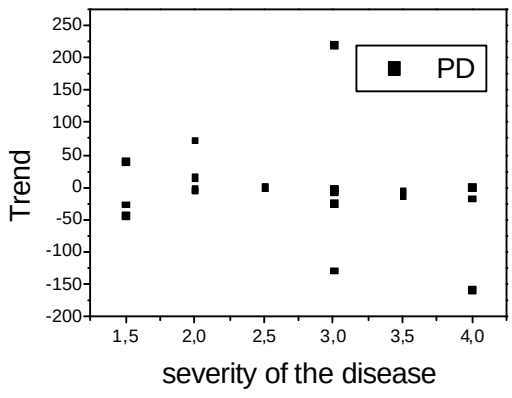

(g.) Trend of PD

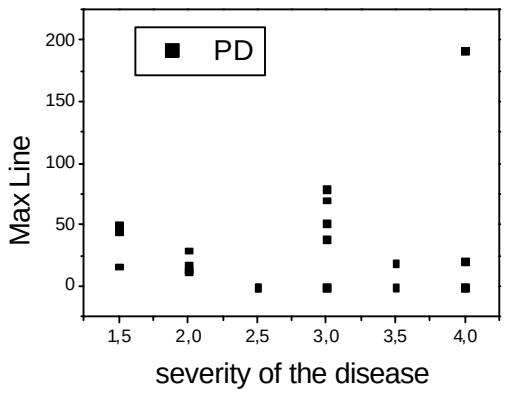

(h.) Max. Line of PD

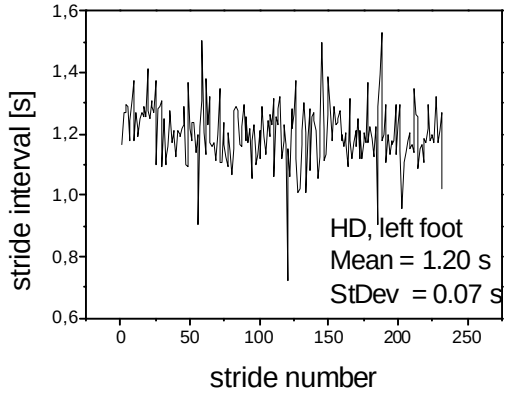

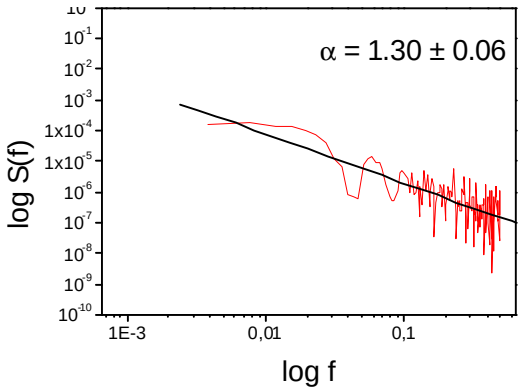

Fig.40. (a.) Time dependence of stride interval (b.) Power fourier spectrum of stride intervals

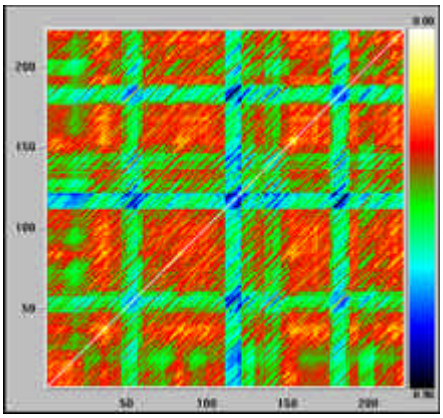

(c.) Recurrence plot of stride intervals

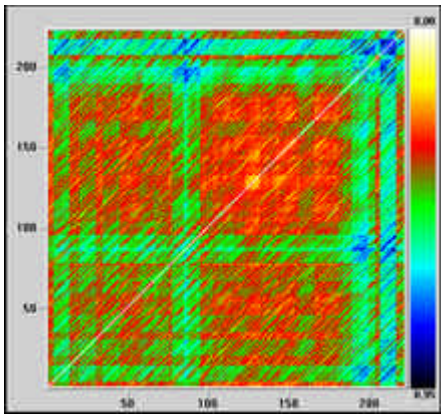

(d.) Randomized recurrence plot

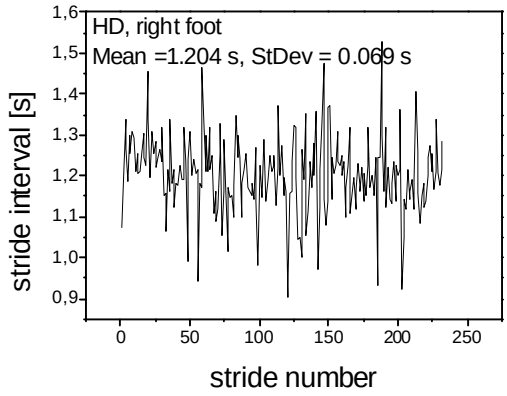

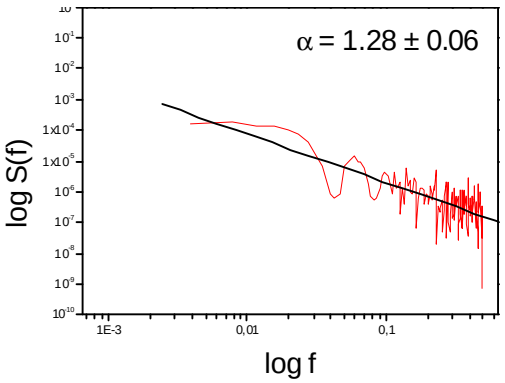

Fig.41. (a.) Time dependence of stride interval (b.) Power fourier spectrum of stride intervals

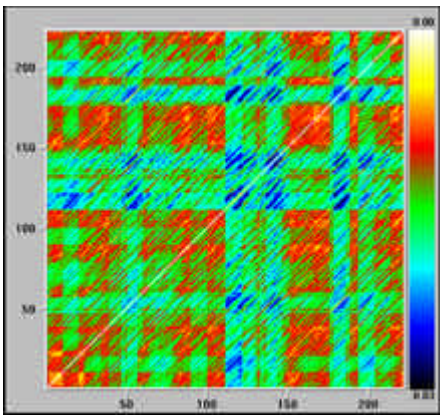

(c.) Recurrence plot of stride intervals

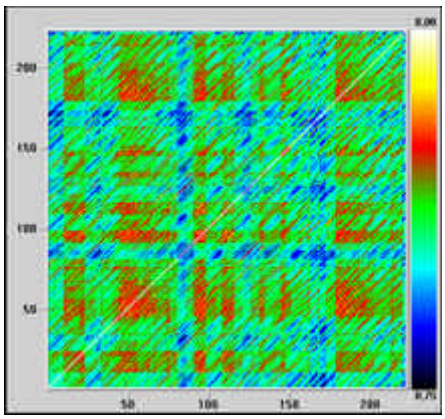

(d.) Randomized recurrence plot

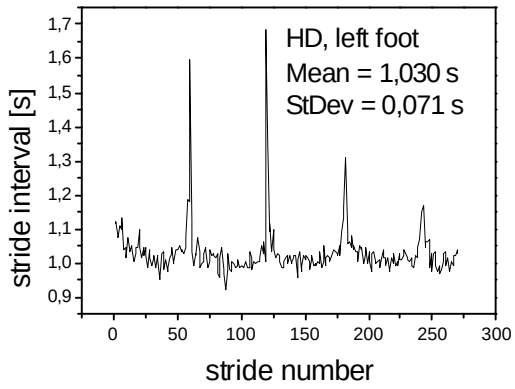

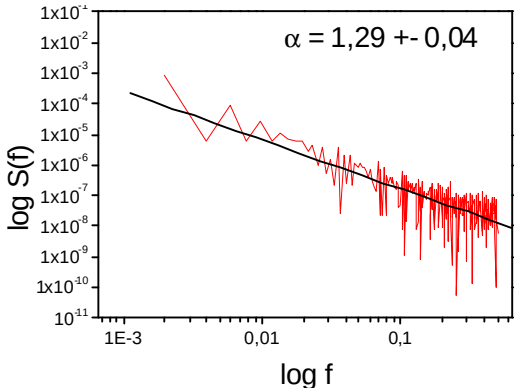

Fig.42. (a.) Time dependence of stride interval (b.) Power fourier spectrum of stride intervals

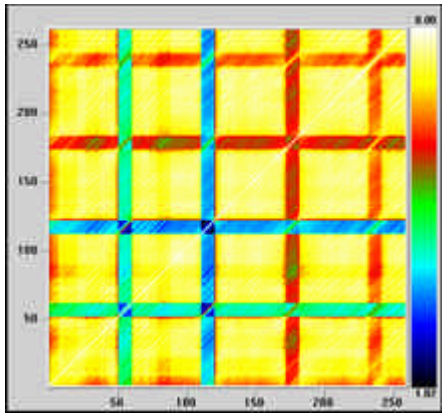

(c.) Recurrence plot of stride intervals

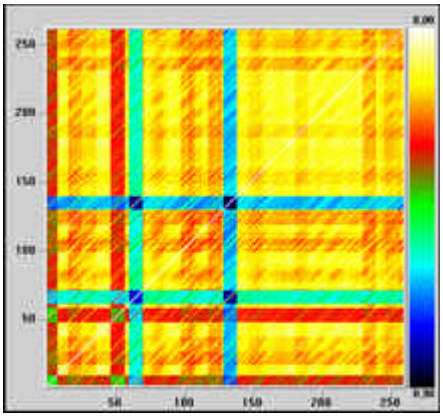

(d.) Randomized recurrence plot

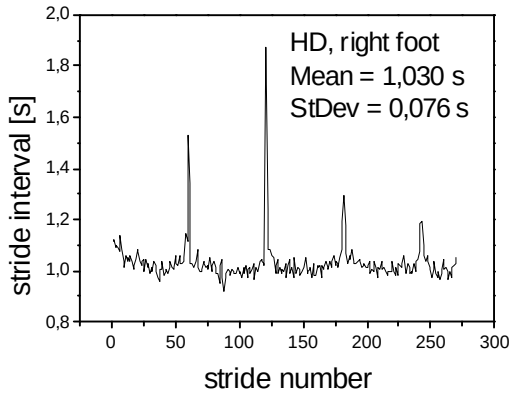

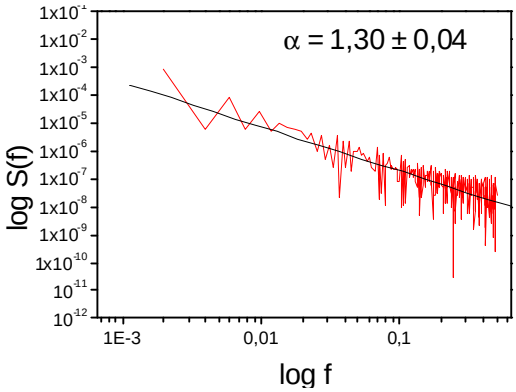

Fig.43. (a.) Time dependence of stride interval (b.) Power fourier spectrum of stride intervals

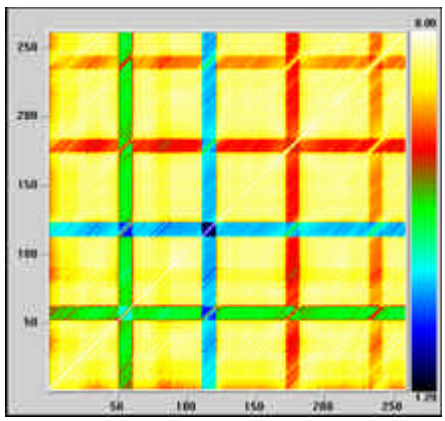

(c.) Recurrence plot of stride intervals

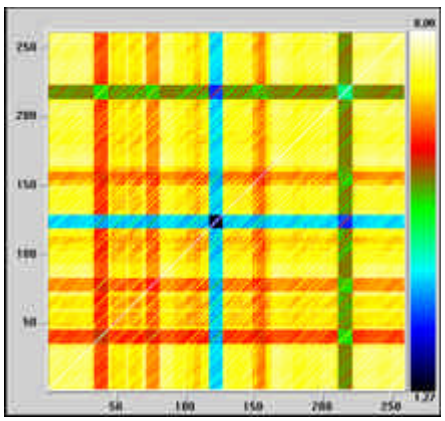

(d.) Randomized recurrence plot

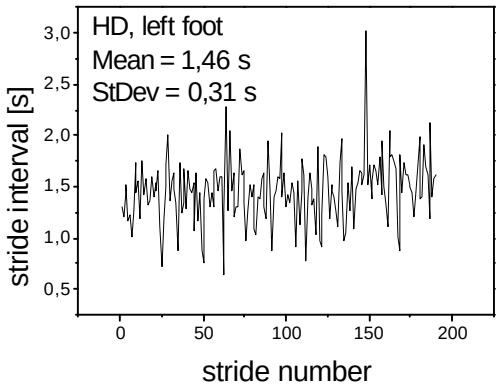

Fig.44.(a.) Time dependence of stride interval

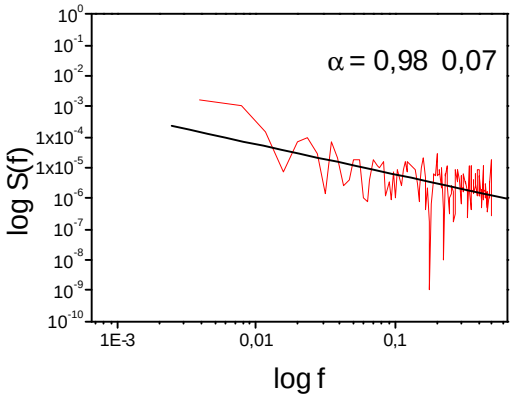

(b.) Power fourier spectrum of stride intervals

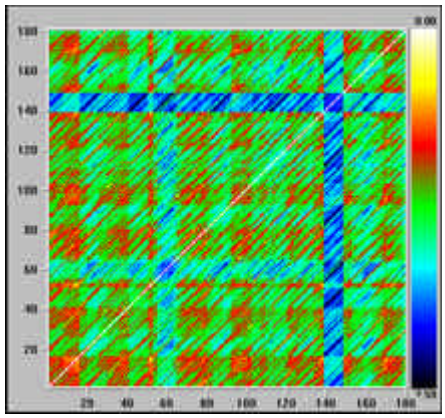

(c.) Recurrence plot of stride intervals

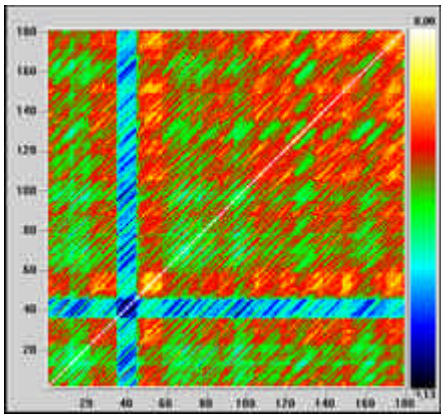

(d.) Randomized recurrence plot

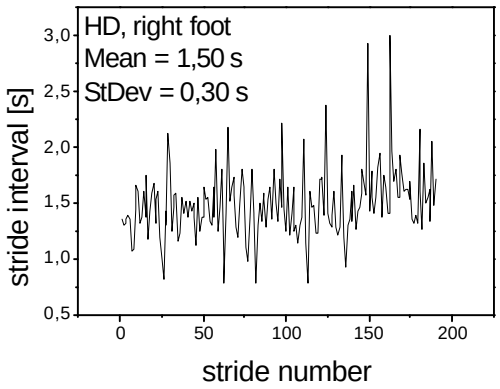

Fig.45. (a.) Time dependence of stride interval

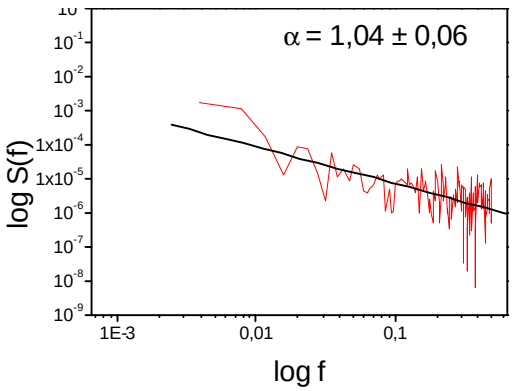

(b.) Power fourier spectrum of stride intervals

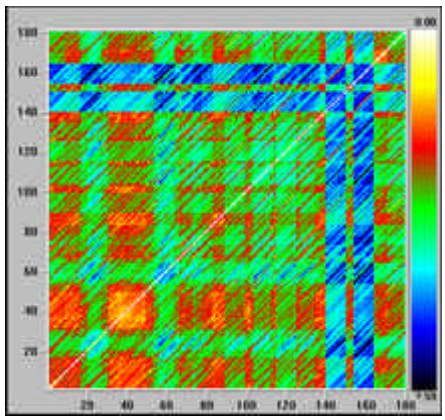

(c.) Recurrence plot of stride intervals

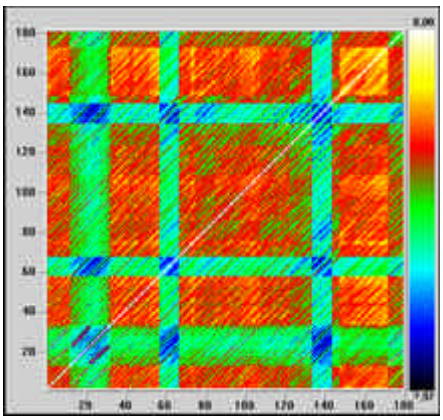

(d.) Randomized recurrence plot

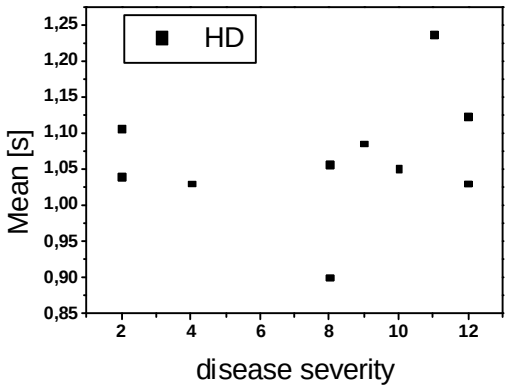

Fig.46. (a.) Mean of stride intervals

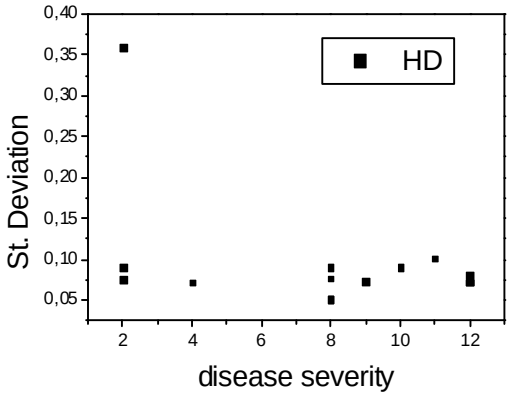

(b.) St. Deviation of stride intervals

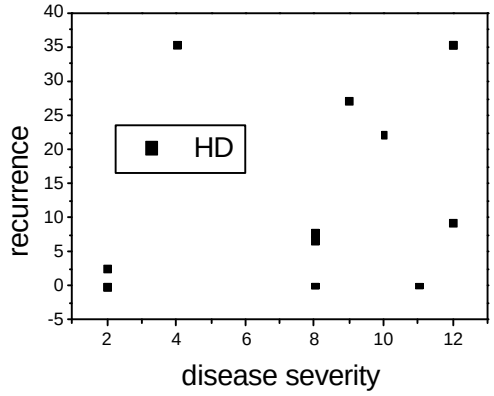

(c.) Recurrence of HD

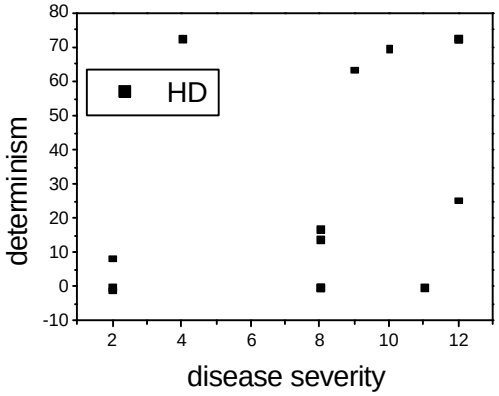

(d.) Determinism of HD

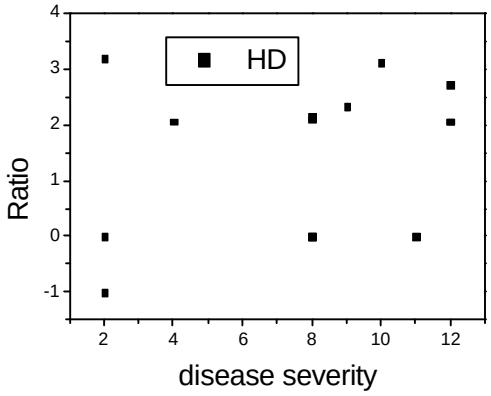

(e.) Ratio of HD

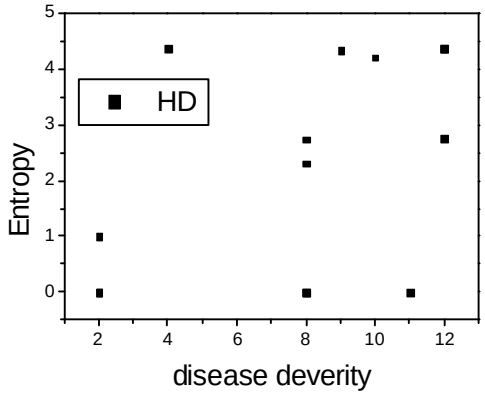

(f.) Entropy of HD

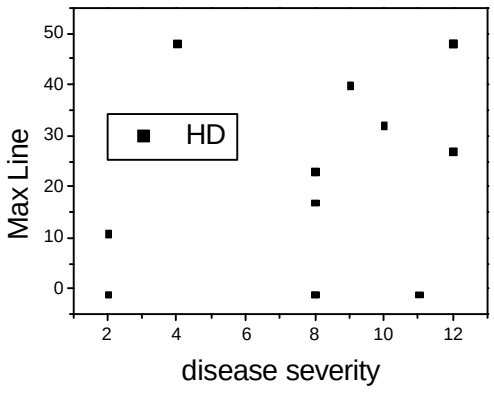

(g.) Max. Line of HD

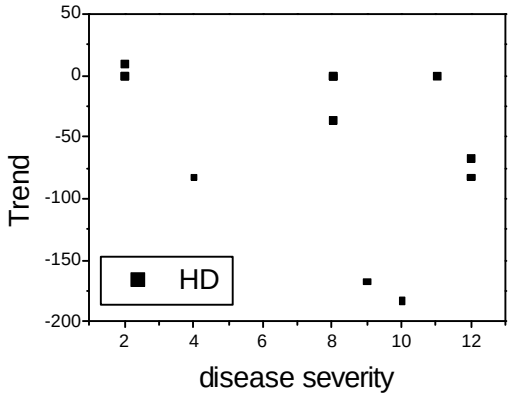

(h.) Trend of HD

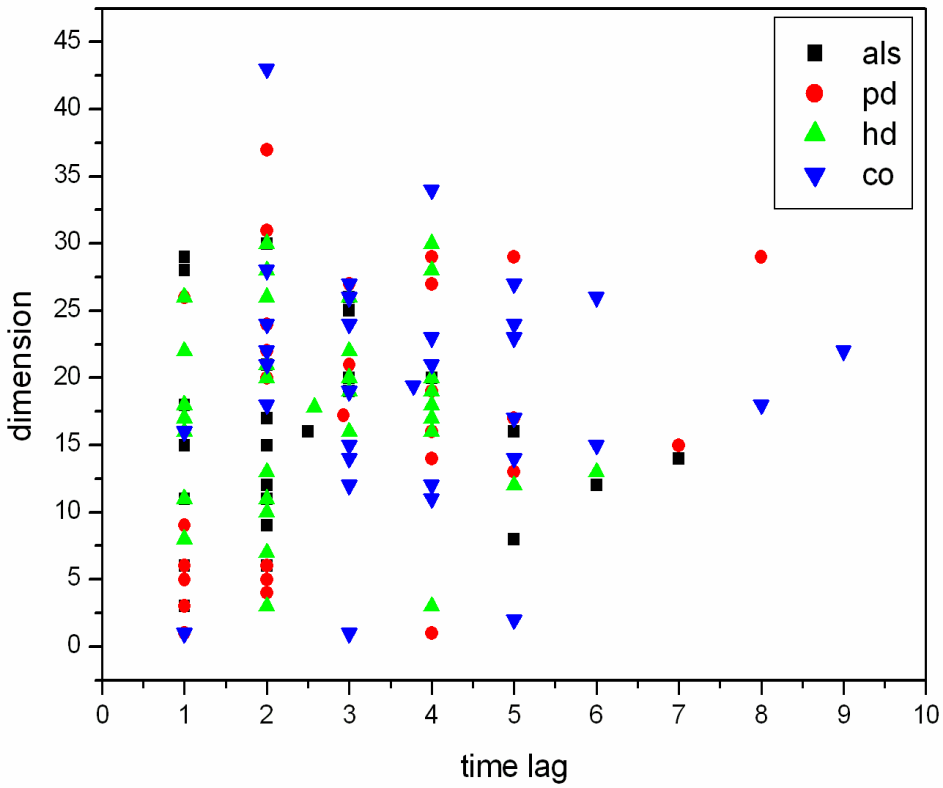

Fig. 47. Embedding dimension in dependence of time lag

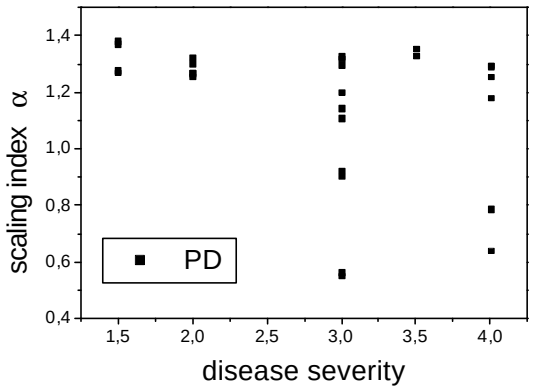

Fig. 48. (a.) Scaling index of PD

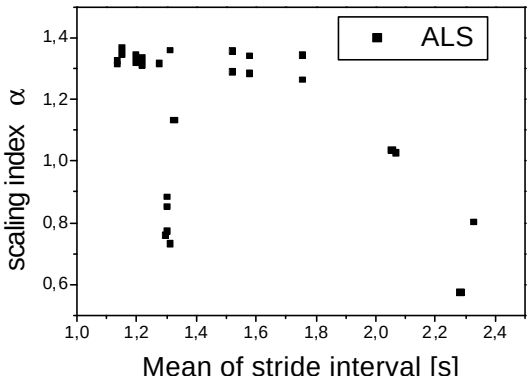

(b.) Scaling index of ALS

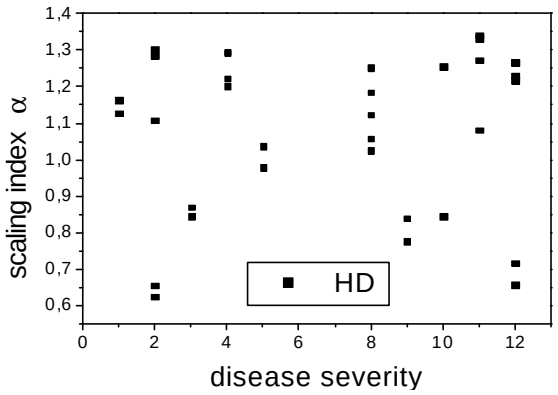

(c.) Scaling index of HD

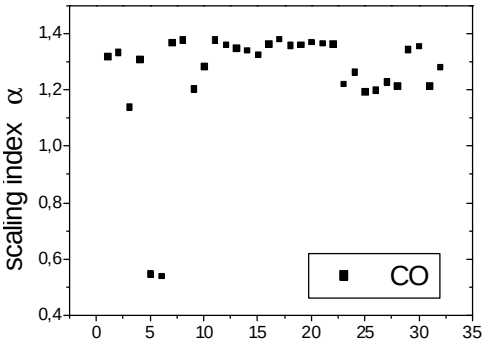

(d.) Scaling index of healthy people

CONCLUSION

This study compares human gait dynamics of children, healthy adults and people with neurodegenerative diseases (amyotrophic lateral sclerosis, Huntington's disease and Parkinson's disease).

The not fully developed locomotor system in children provides changes in gait dynamics. Gait in the youngest children (3-4 years old) is more unstable, with higher fluctuations, in contrast the gait in 13-14 years old children is constant. Also changes in temporal structure measurements are age dependent.The fractal scaling index increases with age and for the oldest children is close to the value of adult people.

From the analysis of recurrent plots and recurrent quatification analysis we can concludes that gait maturation data are mixture of high dimensional daterministic and stochastic processes. With maturation signals become more stochastic.

Gait of people with neurodegenerative diseases shares some common features and is distinguishable from the gait of healthy adult people. There are also distinct attributes among people with ALS, PD and HD which are caused by impairement of different parts of nervous system.

For people with neurodegenerative disease is characteristic increased nonstability, less speed and longer stride intervals. The presence of recurrent patterns in their recurrent plots indicates deterministic structure.

Recurrent plots of stride intervals are empirically correlated with the age and health of the studied subjects, as they diagrammatically represent the complex dynamical interaction of the neuro-muscular systems. These findings suggest that recurrence plots of stride interval variability, show patterns which vary characteristically, for different types of people, in the different states, able to differentiate healthy or ill, old and young subjects.

REFERENCES

[1] Bay J. S., H. Hermani: Modeling of a neural pattern generator with couple nonlinear oscillators, IEEE Trans. Biomed. Eng. 34 (1987) 297-306

[2] Bernstein N., The Coordination and Regulation of Movements, Pergamon, New York, 1935

[3] Casdagli M., S. Eubank, J. D. Farmer, and J. Gibson: State space reconstruction in the presence of noise, Physica D 51,1991, 52.

[4] Eckmann J. P., S. O. Kamphorst, D. Ruelle: Recurrence Plots of Dynamical Systems, Europhys. Lett., 4 (9), 1987

[5] Eckmann J.-P., S. O. Kamphorst, D. Ruelle, and S. Ciliberto: Lyapunov exponents from a time series, Phys. Rev. A 34 (1986) 4971.

[6] Forssberg H., B. Johnels, G. Steg: Is parkinsonian gait caused by a regression to in immature walking pattern?, Adv. Neurol. 40, 1984, 375 – 379

[7] Fraser A. M., H. L. Swinney: Independent Coordinates for Strange Attractors from Mutual Information, Phys. Rev. A 33, 1986

[8] Gabell A., U.S.L. Nayak: The effect of age on variability in gait, J. Gerontol. 39, 1984, 662-666

[9] Goldfarb B. J., S.R. Simon: Gait patterns in patients with amyotrophic lateral sclerosis, Arch. Phys. Med. Rehabil. 65, 1984, 61-65

[10] Grassberger P., I. Procaccia: Measuring the strangeness of strange attractors, Physica D 9, 1983, 189

[11] Hausdorff J. M., L. Zemany, C-K. Peng, A. L. Goldberger: Maturation of gait dynamics: Stride-to-Stride variability and its temporal organization in children, J. Appl. Physiol. 86(3): 1040-1047, 1999 (A)

[12] Hausdorff J. M., S. L. Mitchell, R. Firtion, C. K. Peng, M. E. Cudkowicz, J. Y. Wei, Goldberger: Altered fractal dynamics of gait: reduced stride-interval correlations with aging and Huntington's disease (B)

[13] Hausdorff J. M., A. Lertratanakul, M. E. Cudkowicz, A. L. Peterson, D. Kaliton, A. Goldberger: Dynamic markers of altered gait rhythm in amyotrophic lateral sclerosis, J. Appl. Physiol 88:2045-2053, 2000 (C)

[14] Kantz H.: A robust method to estimate the maximal Lyapunov exponent of a time series, Phys. Lett. A 185, 1994, 77.

[15] Kennel M., Brown R., Abarbanel, H.: Determining embedding dimension for phase-space reconstruction using a geometrical construction. Phys. Rev. A 45, 1992, 3403-3411

[16] Knutsson E.: An analysis of parkinsonian gait, Brain 95 ,1972, 475-486

[17] Koller W. C., J. Trimble: The gait abnormality of Huntington's disease, Neurology 35, 1985, 1450-1454

[18] Muldoon M. R., D. S. Broomhead, J. P. Huke, and R. Hegger: Delay embedding in the presence of dynamical noise, Dynamics and Stability of Systems, 1997.

[19] Rosenstein M. T., J. J. Collins, C. J. De Luca: Reconstruction expansion as ageometry-based framework for choosing proper delay times, Physica D 65, 1993,117.

[20] Sutherland D. H., R. Olshen, E.N. Biden, M.P. Wyatt, The Development of Mature Walking. MacKeith Press. Oxford, 1988

[21]Taga G.: A model of neuro-musculo-skeletal system for human locomotion: Emergence of basic gait, Biol. Cybern. 73 (1996) 97-111

[22] Takens F.: "Detecting strange attractors in turbulence," in Dynamical Systems and Turbulence, Springer-Verlag, Berlin, 1981

[23] Trojan et al.: Fyziologia 2, Osveta, 1992

[24] http://www.lougehrigsdisease.net/

[25] http://www.hdsa.org/

[26]http://www.ninds.nih.gov/health_and_medical/pubs/parkinson_disease_htr.htm#introduction

[27] http://reylab.bidmc.harvard.edu/tutorial/DFA/master.html

[28] http://home.netcom.com/~eugenek/demo.html

RESUMÈ

Predložená práca sa zaoberá porovnávaním dynamiky ľudskej chôdze detí, zdravých dospelých ľudí a ľudí s vybranými neurodegeneratívnymi chorobami.

Dôsledkom poškodenia jednotlivých častí nervovej sústavy zodpovedných za kontrolu pohybu je zmena v dynamike chôdze. Metóda rekurentných obrázkov umožnuje rozlíšit medzi stavom zdravia a choroby. Prítomnost rekurentných vzorov u ľudí s neurodegeneratívnymi chorobami poukazuje na deterministický charakter systému v porovnaní so stochastickým systémom u zdravých ľudí.